12-1-1993

SELECTED TOPICS IN ELECTRIC POWER QUALITY

S. Alyasin
Purdue University School of Electrical Engineering

L. Chung
Purdue University School of Electrical Engineering

D. Hu
Purdue University School of Electrical Engineering

B. Kwon
Purdue University School of Electrical Engineering

A. Risal
Purdue University School of Electrical Engineering

See next page for additional authors

Authors
S. Alyasin, L. Chung, D. Hu, B. Kwon, A. Risal, R. Sasaki, and J. Yang

SELECTED TOPICS IN ELECTRIC POWER QUALITY

S. ALYASIN
L. CHUNG
D. HU
B. KWON
A. RISAL
R. SASAKI
J. YANG

TR-EE 93-50
DECEMBER 1993

SCHOOL OF ELECTRICAL ENGINEERING
PURDUE UNIVERSITY
WEST LAFAYETTE, INDIANA 47907-1285

SELECTED TOPICS IN ELECTRIC POWER QUALITY

S. Alyasin

L. Chung

D. Hu

B. Kwon

A. Risal

R. Sasaki

J. Yang

Purdue Elecmc Power Center

School of Elecmcal Engineering

Purdue University

1285 Electrical Engineering Building

West Lafayette, IN 47907-1285

December 1993

Introduction

Many years ago, I found that the students in EE 532, Computer Applications in Power System Engineering at Purdue University benefited by assembling a "term report". This report is written individually by the students, presented in a videotaped session, and assembled in a written report. For the Fall 1993 semester, the assigned subject was "Selected Topics in Electric Power Quality", and this is the compiled report written by

(Chapter I) Soheil Alyasin
(Chapter II) Reid Sasaki
(Chapter III) Atulya Risal
(Chapter IV) Ling Chung
(Chapter V) Jinyu Yang
(Chapter VI) Brian Kwon
(Chapter VII) Dan Hu.

The topics state with iron core transformers (Chapters I and II), their losses, harmonic response, and connection with electric power quality. Chapter III deals with watt-hour meters and their accuracy in the presence of demand current harmonics. Chapters IV and V deal with two important sources of power quality problems: electric arc furnaces and adjustable speed drives. Chapter VI deals with indices and measurement of electric power quality. The report concludes with a traditional but important topic in electric quality: lightning.

G. T. Heydt
Professor of
Electrical Engineering

December 1993

Table of Contents

Chapter I

Power System Harmonics Associated with Iron Cored Coils

I 1 Introduction

The existence of harmonics in power systems is well documented. The recent surge of interest in electric power quality by the industries signifies the importance of maintaining a low harmonic distortion level in transmission and distribution circuits. In this regard, the IEEE standard 519 is continually revised and improved to set more conservative limits on harmonic distortion and to ensure a high level of power quality.

One known source of harmonics in power systems is the magnetizing current of power transformers. A study of the harmonic levels associated with this phenomenon requires a thorough understanding of the behavior of the transformer core during saturation. Such characteristics are obtained from the B-H curve of the transformer. Thus, a brief explanation of the magnetic characteristics of the iron core during saturation is provided as background information. Once this understanding is established, an analysis of the transient response of the power transformer will be offered. It is important to discuss the fact that transformers are not only a source of harmonics; rather, for practical considerations, they are energized by distorted sinusoids. Thus, a method for realizing transformer core losses due to harmonic content in the energizing element will also be presented.

12 Background

An analysis of transients due to iron cored coils necessitates a good understanding of the magnetic characteristics of the transformer. Consider a winding wrapped around an iron core. Before any current is applied, the iron crystals are as a whole demagnetized. Even at this juncture, small neighboring regions referred to as ***domains*** are magnetized. When an external magnetic field is applied (when the winding is energized), the domains that are aligned with the magnetic axis of the winding will grow. As more current is applied and the field intensity increases, these domains

will continue to grow linearly at the expense of their neighboring atoms. This accounts for the linear portion of the B-H loop. As this situation continues, the aligned domain's ability to take from the unaligned ones decreases and the material goes into saturation. This accounts for the **knee** of the B-H curve and the saturation region.

The B-H **loop** of a ferromagnetic material is obtained by initially demagnetizing the core; then, increasing the current and measuring the field intensity. The corresponding flux density is also measured as field intensity is increased until saturation is reached. At this point, the field intensity is decreased, but it is noted that the return path is **not** along the original trajectory. This accounts for the losses in the transformer core. These losses will later be analyzed as a function of the harmonic content of the source and the amount of flux present as residue in the core at the time of energization.

The phenomenon explained above is essential in studying the harmonics generated by a power transformer during transient periods. These studies are aimed at providing continuous and stable power system operation and are motivated by occurrences such as the disruption in the ***New York*** Power Pool [7] shown in figure **(I. 1).** An autotransformer was energized at Marcy. The harmonic content of the magnetizing current from the saturation of this transformer resulted in a set of capacitor backs tripping 84 miles away at **N.Scotland.**

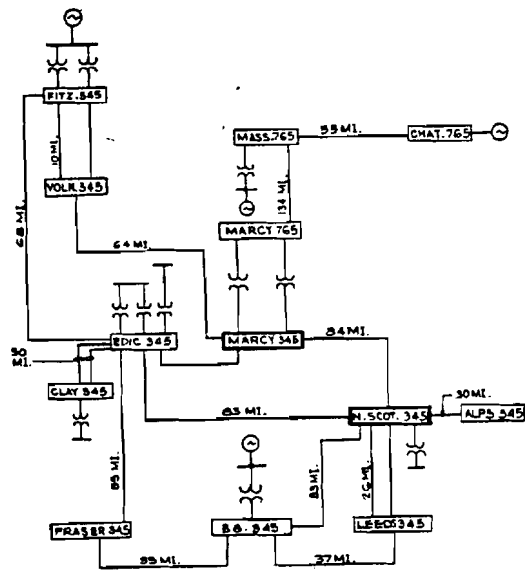

Fig. **(1.1)** - Equivalent circuit of the New York Power Pool

1.3 Harmonic content of the magnetizing current in power transformers under transient conditions

Design of protective systems in transmission and distribution networks calls for an accurate simulation of the transient response in the network. This involves studying phenomenon such as ferroresonance and inrush currents. Ferroresonance, however, yields distortion at frequencies lower than the power frequency and in this regard does not belong in a study of harmonics due to transformer saturation.

When a transformer is energized, a surge of current rich in harmonics, known as the magnetizing inrush current, flows for a short period of time until normal flux conditions are established. The magnitude of this current is a function of the magnitude and phase of the energizing voltage as well as any flux residue that may be present in the core. Figure (1.2) provides a qualitative view of what occurs. If at the instant the source is switched on to the transformer, the voltage has zero phase, the core experiences a full half cycle of positive voltage capable of driving it to saturation on the B-H curve (point A in figure (1.2)). However, if the voltage is at a phase of 90 degrees, only a half cycle of positive voltage feeds the core, and very little if any saturation is expected (point B in figure (1.2)).

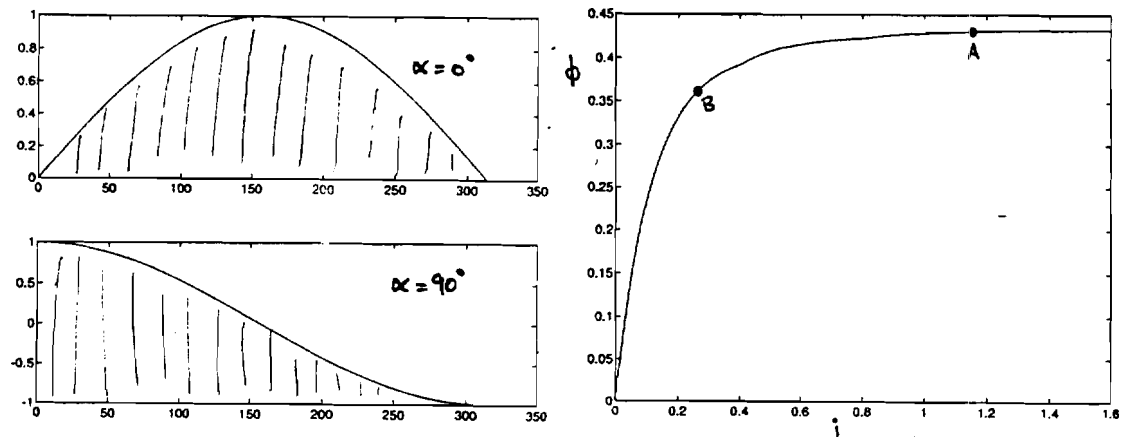

Fig. (1.2) - Affect of the Phase of the Voltage Source on Inrush

The inrush phenomenon is verified by laboratory experimentation. The circuit shown in figure (I.3a) was constructed. For different switching trials (different phase angles of the voltage source), the current on the primary side of the transformer (marked X1) is observed and it is verified that the magnitude and direction of inrush current is directly related to the phase of the voltage source at the moment of energization. Figure (I.3b) shows a few cycles of the inrush current for each case.

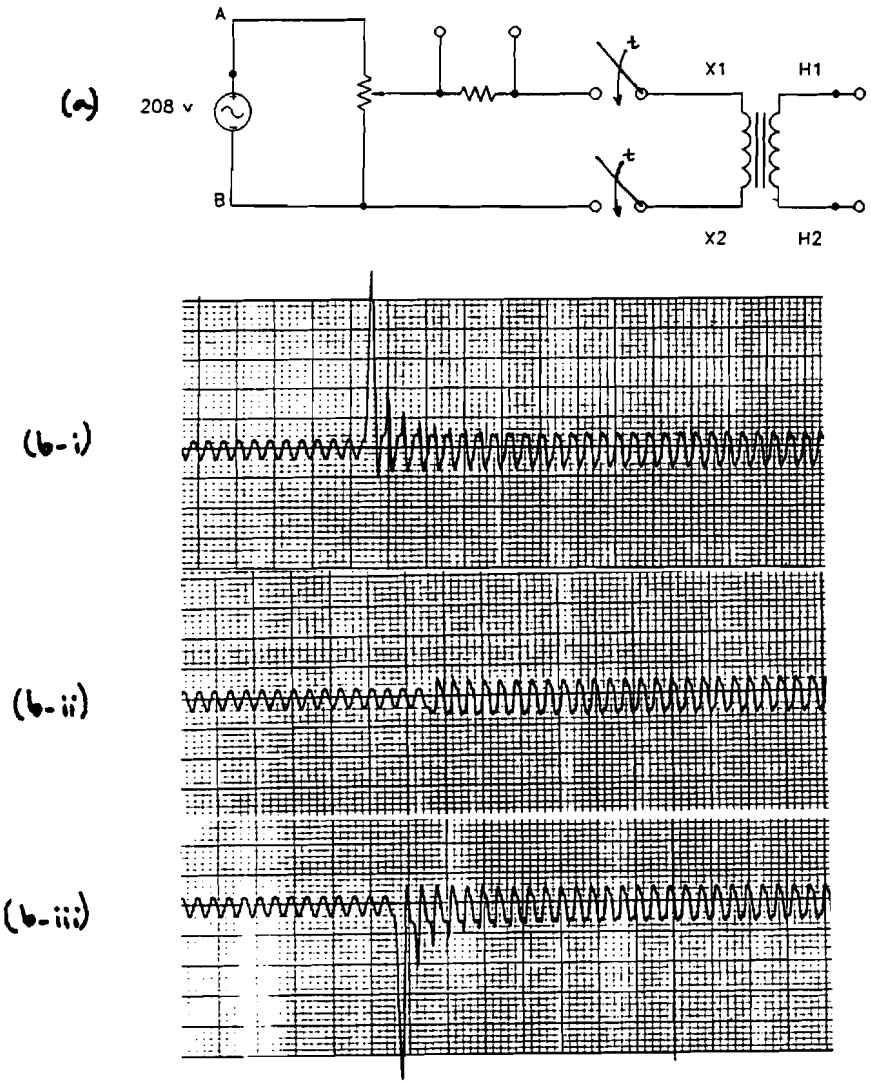

Fig. (I.3) - (a) Circuit diagram to test inrush current phenomenon
(b) Results verifying inrush dependency on voltage phase
(3b-i) large positive inrush signifying approx. a zero phase
(3b-ii) no inrush signifying approx. a ninety degree phase
(3b-iii) large neg. inrush signifying approx. phase > 90 deg.

For the purpose of providing a quantitative study of the inrush current phenomenon, the algorithm developed by M. Basu[1] has been employed. The circuit diagram is shown below.

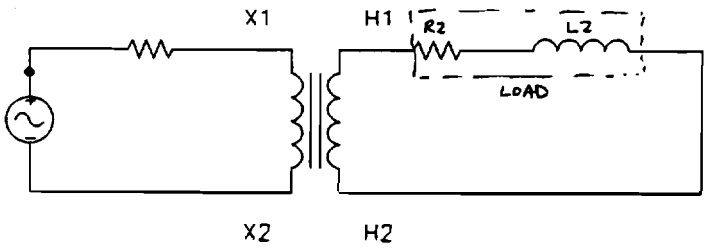

Fig. (I.4) - Circuit for Inrush Simulation

This algorithm neglects hysteresis and Eddy current losses. Eddy current losses can easily be incorporated by placing a resistor (often denoted Re) in parallel with the magnetizing inductance. Hysteresis losses are mainly a concern when residual flux is present. For the case simulated, no residual flux is present, therefore these losses can be neglected. Also note that the leakage components on the secondary side of the transformer are included as part of the load. The transformer core data needed for the simulation are shown in Figure(I.5). They are approximated as shown by Jwa [3].

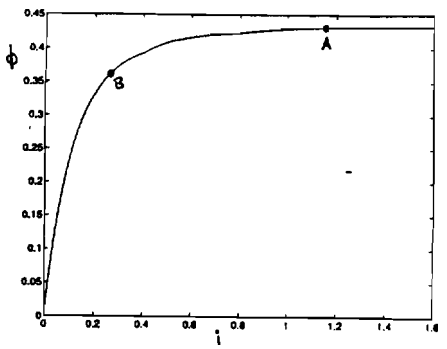

Fig. (1.5) - flux vs. current curve for simulated transformer

Figure (I.6) shows the inrush current with no phase shift (figure(I.6a)), a phase shift of 45 degrees (figure(I.6b)), and a phase shift of 90 degrees (figure (I.6c)). The following results are for a full load case with R2=3.2Ω and L2=5mH. Note the changes in the dc component for the three different cases.

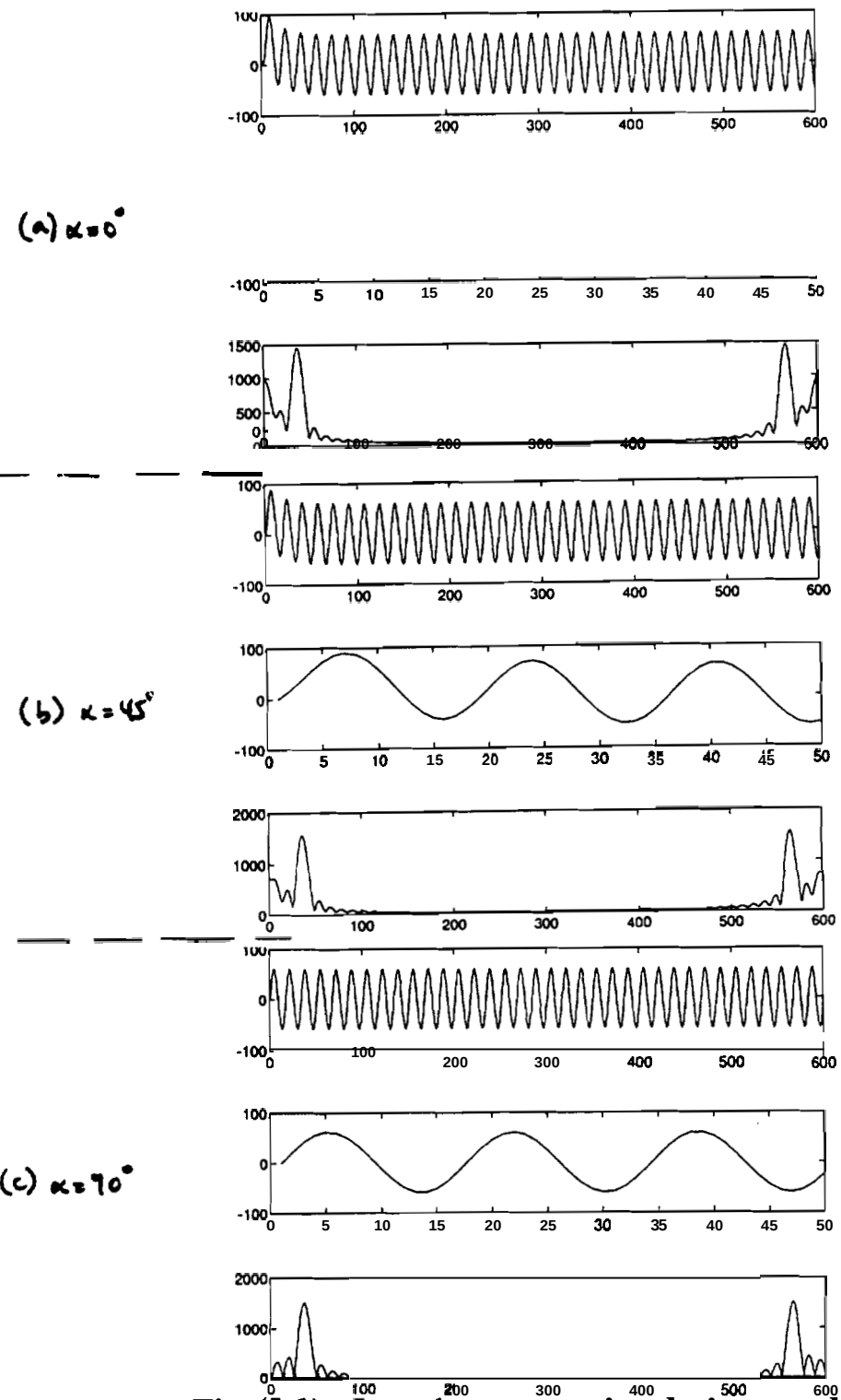

Fig. (I.6) - Inrush current simulation results
(I.6a) - top: closing angle of 0 degrees
(I.6b) - middle: closing angle of 45 degrees
(1.6c) - bottom: closing angle of 90 degrees

It is important to mention the fact that the term ***harmonics*** is exclusively used to refer to the frequency domain representation of periodic time functions at frequencies which are multiples of the fundamental frequency (60Hz for power purposes in the U.S.). Inrush currents are not periodic and in a strict sense can not have harmonics. Thus, any mention of inrush current harmonics refers to peaks found at harmonic frequencies by performing a windowed FFT at segments of interest in the current waveform.

To consider other loading conditions, results simulated by Lin et. al[4] are presented. This data is based on a closing angle of zero degrees for worst case results. For an unloaded transformer (figure (I.7)), a comparison of the two diagrams shows that the presence of positive residual flux in the core for positive inrush current results in a larger harmonic at dc. The unloaded transformer case provides the largest inrush. For a transformer with a resistive load (figure (I.8)), inrush harmonics are smaller than before. Furthennore, the larger the resistance, the more the circuit resembles an open circuit condition greater inrush peaks are viewed. For an inductive load (figure(I.9)), inrush is less than for a resistive one. Furthermore, as pf increases for this type of loading, although Lin's results don't clearly show this, an increase in inrush is expected. For a capacitive load (figure(I.10)), inrush is greater than for a resistive case and inrush decreases for an increasing pf.

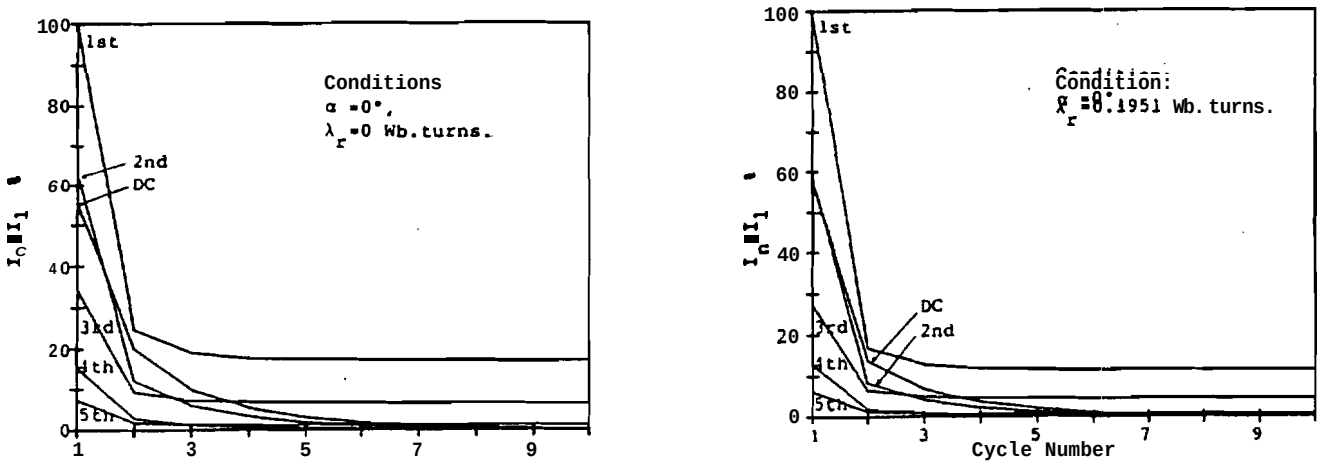

Figure (1.7) - No load condition
(a) residual flux=0
(b) residual flux=0.1951 wb-t

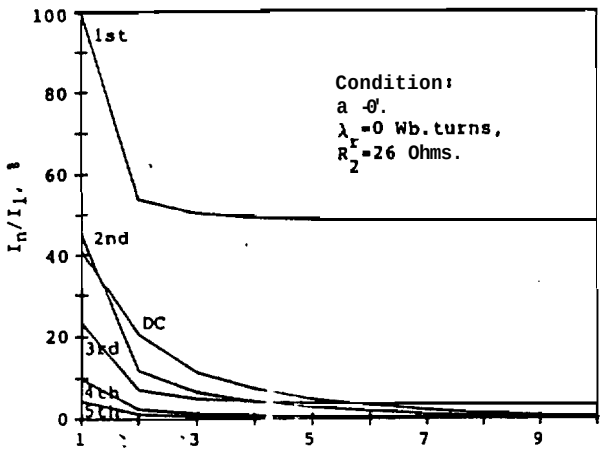

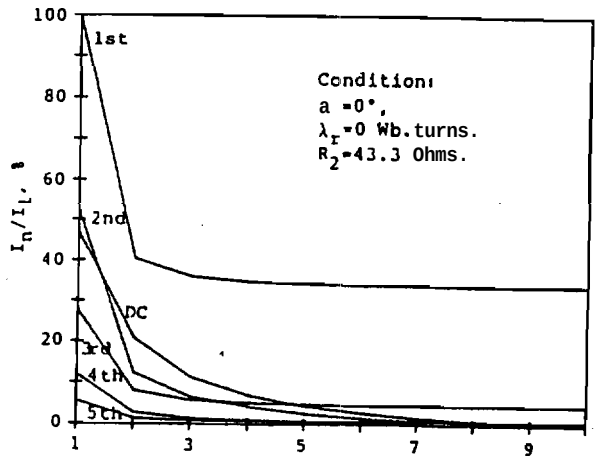

Figure (I.8) - Resistive load
(a) R=26Ω
(b) R=43Ω

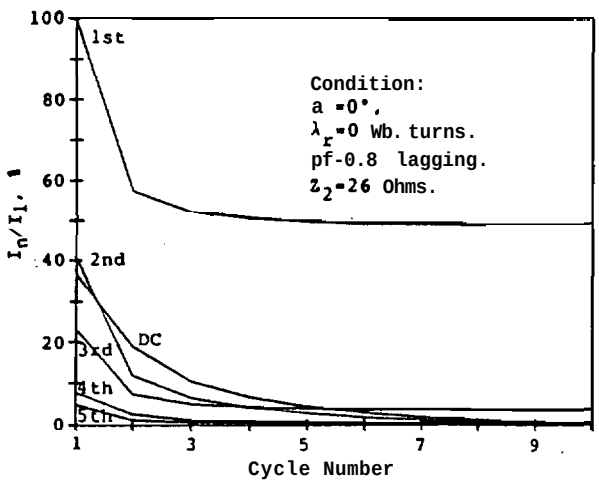

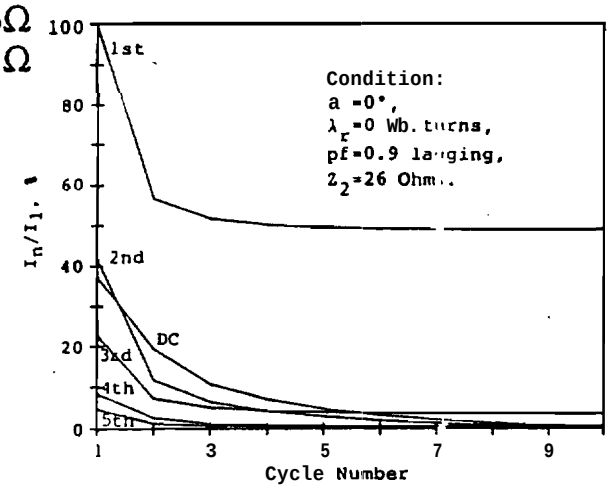

Figure (1.9) - Inductive load
(a) pf=0.8 lagging
(b) pf= 0.9 lagging

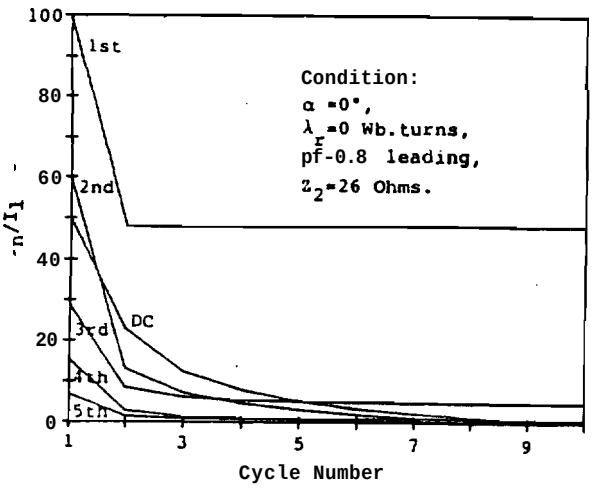

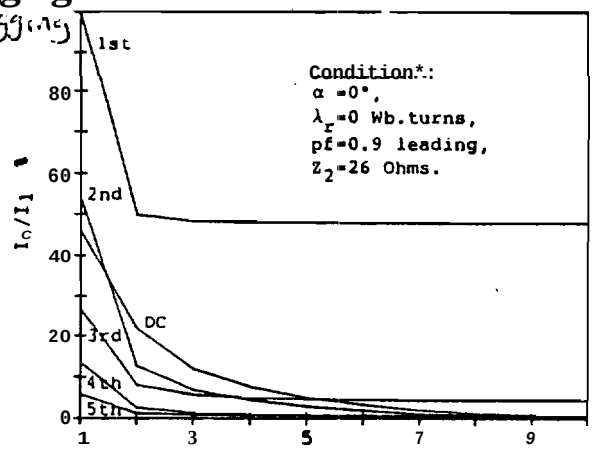

Figure (1.10) - Capacitive load
(a) pf = 0.8 leading
(b) pf=0.9 leading

1.4 Transformer core losses due to harmonic components in the energizing waveform

Traditionally, the inrush phenomenon of power system transformers has been analyzed by assuming a sinusoidal energizing element as discussed above. For practical applications this is often not the case. For example, consider a distribution transformer at the end of a transmission line. The receiving end voltage used to energize the transformer is not a perfect sinusoid because it gets distorted by the reflections of the harmonics generated from the saturation of the transformer.

The above statements provide motivation for the development of a method to determine the core losses due to harmonic flux components. A method has been proposed by Rupanagunta[7]. This method is applicable when a transformer is energized with a distorted waveform. If the harmonic levels are known, the transformer losses for each harmonic can be realized.

This method is based on the importance of flux density vs. time (B(t)) waveforms in assessing losses due to harmonic components. Without considering these flux density waveforms, simple mathematical addition of core losses due to each harmonic component from manufacturer's data may result in an inaccurate calculation of losses. This is realized by observing figure (1.11). In part (a), the third harmonic component is in phase with the fundamental. In part(b), the third harmonic lags the fundamental by 90 degrees. It is clear that the resultant flux density is very different for the two cases. Thus, one must analyze the shape of the flux density curve in order to be able to accurately assess losses in the transformer core.

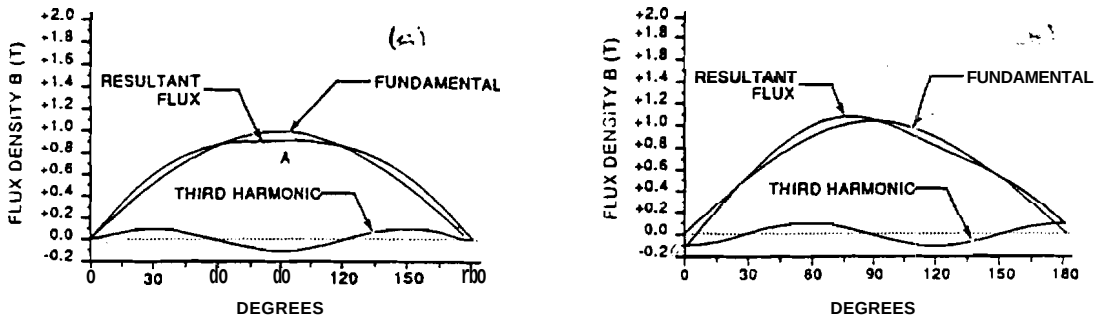

Fig. (1.11) - Flux density vs. time
(a) third harmonic in phase with fundamental
(b) third harmonic lagging fund. by 90 degrees

The following equations can be used to determine the flux density. From Faraday's Law:

$$v(wt)=n\frac{d\phi}{d(wt)}$$

where $\phi = BA$

Thus, the flux density is denoted by:

$$B=K\int v(wt)d(wt)$$

K= proportionality constant
v(wt)=back EMF across winding
w=angular freq. of exciting EMF
B=flux density in material

For a general case, the distortion voltage is expressed by the following Fourier Series:

$$v(wt)=v1(\sin[wt+\theta 1])+v3(\sin[3wt+\theta 3])+...$$
$$+v(2n+1)(\sin[(2n+1)wt+\theta(2n+1)])+...$$

n=1,3,5
Vn=nth harmonic back EMF across the winding
Theta n= phase angle in radions for the nth harm. comp.

The flux density is then expressed as:

$$B(wt)=K\{-v1(\cos[wt+\theta 1])-v3/3(\cos[wt+\theta 3])+...$$
$$-v(2n+1)/(2n+1)(\cos[(2n+1)wt+\theta(2n+1)])+...$$

The following data must be available to employ this method:

B-H loop at fundamental frequency
B-H loop at harmonic frequency of interest
dc hysteresis loop

If the above is not provided in the manufacturer's data charts, Rupanagunta proposes the following algorithm. A three phase transformer circuit is formed such that the primary is y-connected and secondary is

delta connected. The primary is fed by a balanced three phase 60Hz voltage. The harmonic of interest (in this case third) is applied to the secondary. The delta connection allows for zero sequence or one phase current flow. The balanced three phase fundamental emf applied to the primary results in no induced emf in the secondary since the fundamental frequencies sum to zero. Furthermore, by leaving the neutral of the fundamental frequency coils isolated from the power supply neutral, the y-connection is an open circuit as far as the third harmonic circuit is concerned. By isolating the harmonic components, the B-H loops can be obtained at fundamental or 180Hz separately.

Experimentally, it has been observed that in the presence of harmonic components in the energizing voltage, the B-H loop experiences inner loops. It is observed that in the (B vs. time) waveform, for dB/dt=0, if two values of B are present, incursions are observed in the B-H loop. These incursions are the starting points of the inner loops and are depicted below:

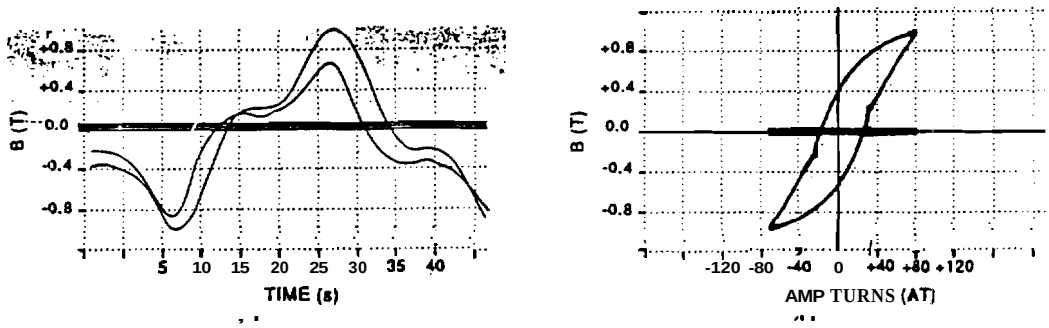

Fig. (1.12) - Incursions in the B-H loop

This method can be used to determine the number, magnitude, and position of the inner loops. The vertical bounds of the minor loops is directly proportional to the magnitude of the secondary peak as shown below.

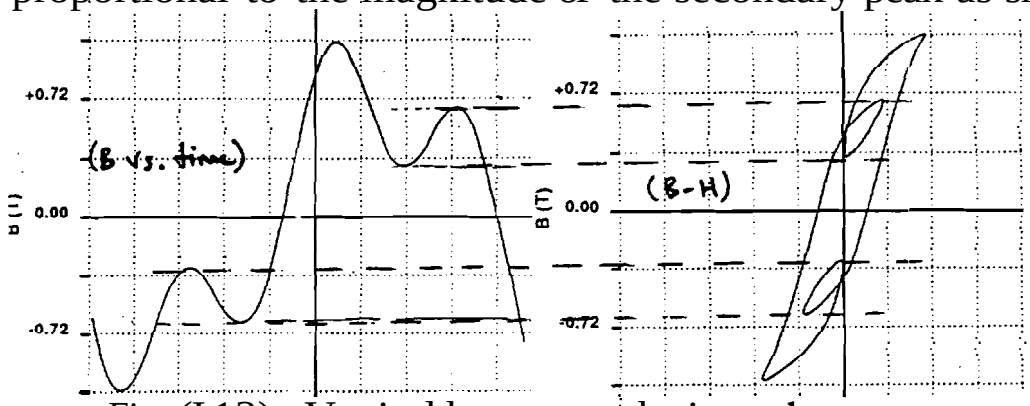

Fig. (I.13) - Vertical bounas or the inner loops

The width of the minor loops can be determined by first selecting a B-H loop from the family of 180Hz curves that has the same height as the length from the lowest point on the third harmonic content of the B(t) waveform to the highest component of this function. This is shown below in figure (1.14).

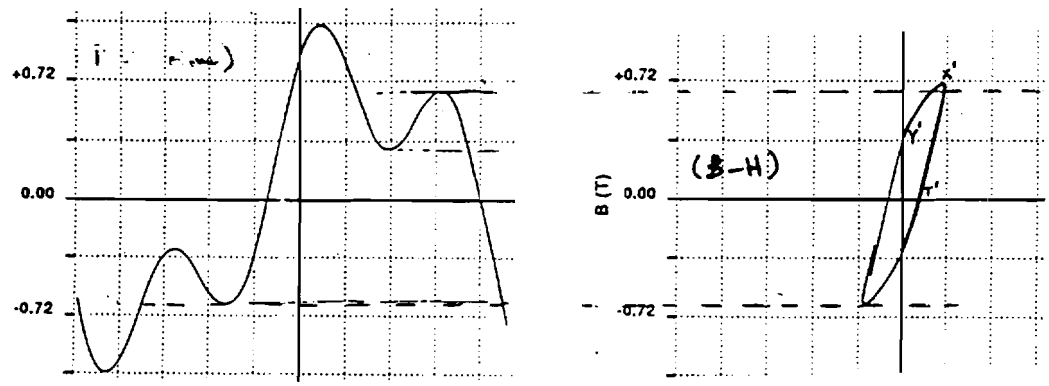

Fig. (I.14) - Selection of an appropriate 180Hz B-H loop

This B-H loop is placed in the main loop such that points M and N fall on the H=0 AT axis where the 180Hz loop crosses that axis. Points G and R are the incursion points found by the method already mentioned. Point X is connected to point F by interpolation along the inversion point G. M is connected to the peak of the B-H loop by interpolation along G. The M to X curve is extrapolated form the Y'X'T' contour in the 180Hz B-H loop shown in figure (1.14). Assuming that B(t) is symmetric about the time axis, the other minor loop is simply sketched by symmetry. This is observed in figure (I.15).

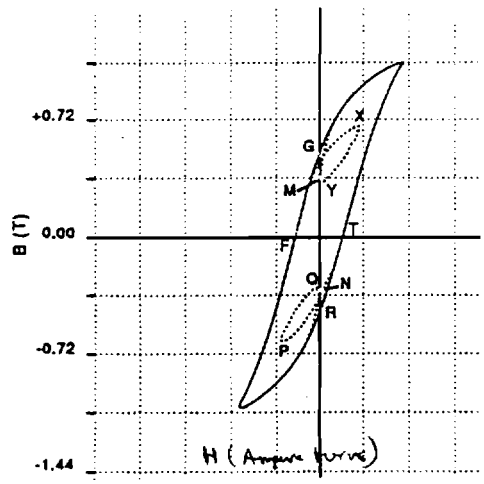

Fig. (I.15) - Determining the dimensions of the inner loops

The minor loops in the **B-H** curve may be found using this method for any harmonic component of interest. Research is being carried out to expand this method such that it can be used to find minor loops due to many different harmonics in the energizing elements.

The hysteresis and eddy current losses in the transformer core can be separated by placing the dc hysteresis (static) loop in the **B-H** curve of figure (I.15). The inner loop (dc) contains the hysteresis losses. The outer contains the total losses. The difference of the two composes the eddy ***current*** losses. This is viewed in figure (I.16).

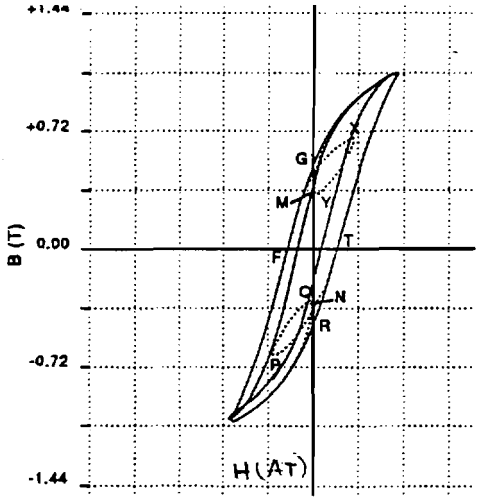

Fig. (1.16) - Separating hysteresis and eddy current losses

15 **Conclusion**

The major points of the above discussion are listed below.

The harmonics associated with energizing a power transformer have been identified. Harmonics due to inrush currents are affected by the following factors:

- Phase of the energizing voltage at instant of **switching: maximum** pos. inrush for zero phase. This decreases until 90 degree phase. **Past** 90 degrees, the inrush current increases in the negative direction.
- Largest inrush harmonics are seen in unloaded transformers
- Resistive load results in smaller harmonics than no load – the larger the resistance, the larger the harmonics on the primary side current.

- Lagging pf loads (inductive) result in lower harmonic levels than resistive loads.
- Leading pf loads (capacitive) result in higher harmonic levels than resistive loads.
- For an inductive load, increase in pf increases inrush.
- For a capacitive load, increase in pf decreases inrush.

The voltages used to energize transformers are seldom perfectly sinusoidal. Thus, a method to realize the effects of the distorted voltages on the transformer core has been discussed. The significant points made are as follow

- Simply summing the core loss data from manufacturer's charts without observing the exact form of B vs. time yields inaccurate results.
- The position and number of inner loops in the B-H curve is determined from the form of the B vs. time waveform.
- The width of the inner loops is obtained using the contour of the B-H curve at the harmonic frequency of interest.

16 References

[1] Basu, M. and Basu, K.P. "Computerized Evaluation of the Magnetizing Inrush Current in Transformers." Electric Power Systems Research. Vol.2 (1979) pp. 179-182.

[2] Heydt, G.T. Electric Power Quality. Stars in a Circle Publications: West Lafayette, IN 1991.

[3] Jwa, C.K. and Ong, C.M. "Method of Predicting Inrush. Current in Transformers." Industry Application Society. Conference Proceedings, 1985.

[4] Lin, C.E. et al. "Investigation of Magnetizing Inrush Current in Transformers. Part II- Harmonic Analysis." IEEE Trans. on Power Delivery. Vol. 89, No.1, Jan 1993. pp255-263.

[5] MIT, faculty of. Magnetic Circuits and Transformers. John Wiley and Sons: NY. July 1950.

[6] Ray, S. "Analysis of Transient Behavior of Power System Circuits Containing Iron Cored Coils." IEEE Proceedings. Vol 138, No.4, July 1991. pp275-282.

[7] Rupanagunta, et. al. "Determination of Iron Cored Losses Under Influence of Third Harmonic Flux Component." IEEE Transactions on Magnetics. Vol 27, No.2, March 1991. pp768-777.

[8] Viviani, G.L, and Li, L. "A Transformer Model for Investigating the Effects of Harmonics." Proceedings of ICHPS-III. Nashville, IN 1988. pp149-154.

CHAPTER II
LOSS OF DISTRIBUTION TRANSFORMER LIFE

Reid I. Sasaki

II.1 Introduction

The distribution transformer is an integral part of a power system network. It is instrumental in transforming distribution line voltage down to the service voltage required by the customer. The transformer itself is a device dependent specifically on its magnetic characteristics therefore it is vulnerable to the limitations of the core material. These limitations manifest themselves in the form of hysteresis losses as well as eddy current losses in the core and windings. These losses are dissipated as heat in the transformer and result in dielectric and insulative breakdown which significantly reduce the operational lifetime of the transformer.

The combined factors of increased demand of power from domestic users and industry along with the utilization of solid state switching devices have greatly decreased the life expectancy of distribution transformers. This is due to the relatively large harmonic current imposed on the distribution transformer.

The Institute of Electrical and Electronics Engineers (IEEE) has recognized the problem of increased losses in distribution transformers due to nonlinear loads and has established a recommended practice for the derating of distribution transformers when supplying nonsinusoidal load currents.

II.2 Description of Distribution Transformer Losses

The vast majority of power transformers used for distribution applications are of core-type construction. This consists of the high-voltage (primary) and low-voltage (secondary) windings of the transformer wound concentrically around a magnetic core of rectangular or circular cross-section, which is shown in Fig. 11.2-la. The core assembly may either be free-standing or

surrounded by a metal enclosure, which is referred to as a dry-type transformer, or immersed in oil within a steel tank. A oil-immersed distribution transformer typical of rating from 2 to 25 kVA 7,200 V:240/120 V is shown in Fig. 11.2-lb. [1]

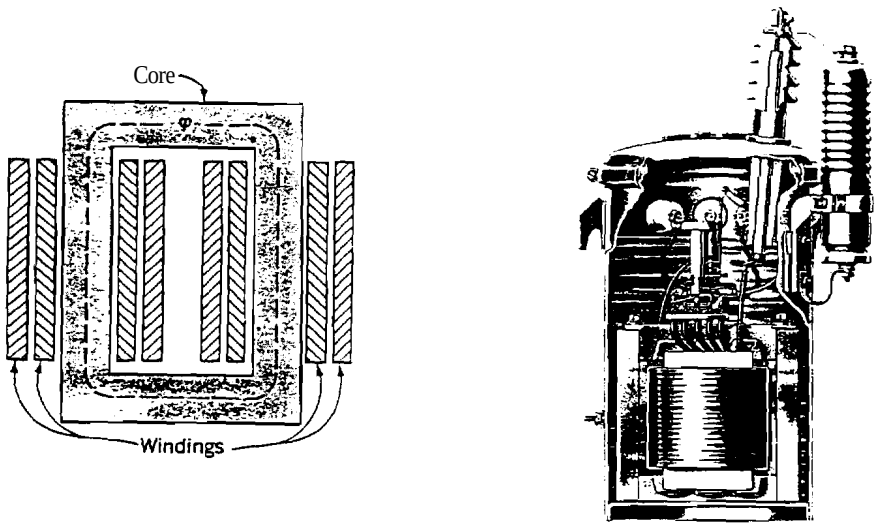

Fig. 11.2-1 Distribution Transformer. (a) Core-construction; (b) cross-section.

Transformer losses can be divided into no-load (excitation) losses and load (impedance) losses which are dissapated as heat in the transformer. No-load losses are incurred in the magnetic core of the transformer when an time-varying exciting current is applied to primary winding to produce a magnetic field within the core. Load losses are incurred in all metallic conductors of the transformer and are due to the load current flowing in the primary and secondary windings. Both types of losses are described in detail below.

No-load losses in the transformer are primarily due to the nonlinear properties of the magnetic material used for the core of the transformer. The magnetic core serves to provide a low reluctance path for the mutual flux coupling the primary and secondary windings and also to reduce the excitation current required for transformer operation. When an time-varying excitation current is applied to the primary windings of the transformer, a proportional magnetic field H is induced in the core. Because the core is magnetic, a flux density B is produced which is proportional to H by a effective permeability constant μ of the core material. Because the relationship between B and H is nonlinear and multivalued, it is usually shown in graphical form referred to as a B-H curve or hysteresis loop.

The equivalent T-circuit for a transformer is shown below in Fig. II.2-2. It is noted that the primary current **I,** can be resolved into a load component and an exciting component. The load current I,' is defined as the current drawn by the load connected to the secondary winding of the transformer while the excitation current $I\varphi$ is defined as the additional primary current required to produce the mutual flux φ coupling the primary and secondary windings. **A** curve of $i\varphi$ versus time can be obtained from the *B-H* characteristic of the core material since $\varphi = BcA$ and $i\varphi = Hclc/N$ (where *Ac* is the cross-sectional area of the core, *Ic* is the mean core length, and Nis the number of turns of the primary winding.) This is shown below in Fig. II.2-3. [1]

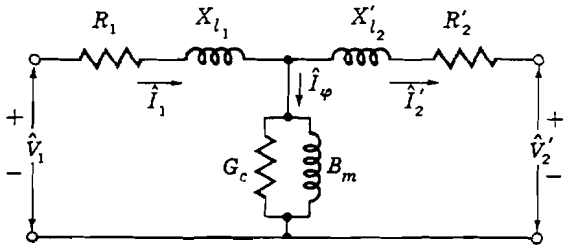

Fig. II.2-2 Equivalent T-Circuit for a Transformer

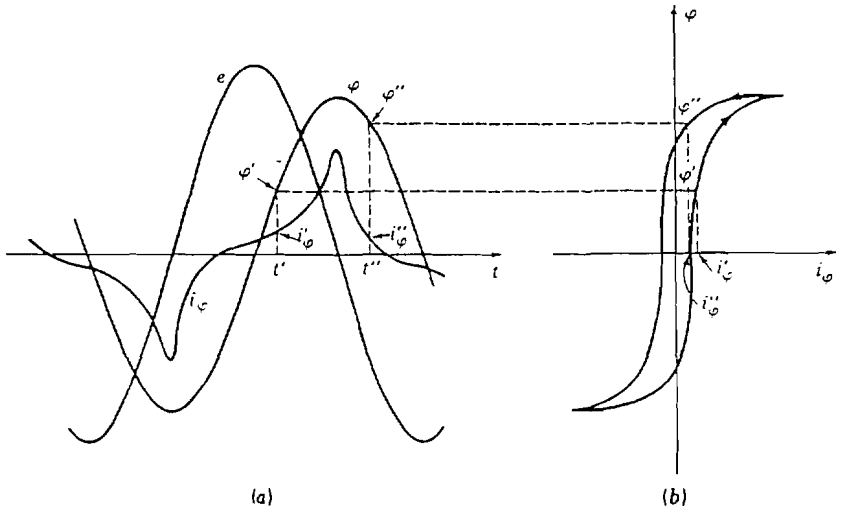

Fig. II.2-3 Excitation phenomena. (a) Voltage, flux, and exciting current; (b) corresponding hysteresis loop.

The excitation current $I\varphi$ can be further resolved into a core-loss component and a magnetizing component. The core-loss component I_c is defined as the eddy currents induced in the core and appear as ohmic I^2R heating in the transformer. These eddy currents circulate in the core and oppose the change of flux density. To oppose this demagnetization effect, the current in

the exciting winding must increase, thus enlarging the area enclosed by the hysteresis loop. The losses due to eddy currents, which are dissipated as heat in the transformer, are often reduced by constructing the core of thin sheets of laminations of magnetic material which are aligned in the direction of the field lines. These sheets are insulated from each other by a layer of oxide or enamel and greatly reduce the magnitude of the eddy currents by interrupting its path in the core material.

The magnetizing component I_m is defined as the current required to magnetize the core material. This time-varying excitation current will cause the magnetic core material to undergo a cyclic variation, creating a hysteresis loop. The energy input to the core for a single cycle can defined as $W = Aclc \oint Hc \bullet dB$ (where W is the energy applied to the core, Ac is the cross-sectional area of the core, and lc is the mean core length.) Energy loss due to hysteresis is therefore proportional to the volume of the core $Aclc$ and the are enclosed by the hysteresis loop $\oint Hc \bullet Bc$. Since there is an energy loss per cycle, hysteresis power loss is proportional to the frequency of the applied excitation current and is dissipated as heat in the transformer. [1]

Load loss of a transformer can be subdivided into I^2R loss and "stray loss". I^2R loss is defined as the loss due to the dc resistance of the primary and secondary windings. When a direct current is applied to the windings, the temperature of the winding conductors increases and is dissipated in the form of heat in the transformer. Stray loss is defined as the loss produced by time-varying load currents flowing in the windings of the transformer. The alternating currents produce stray electromagnetic fields which encircle the windings. A picture of the electromagnetic fields produced by rated load current for a typical transformer is shown in Fig. II.2-4. These fields in turn link 'the windings, the core, the enclosure, anal other metallic conductors of the transformer. Each of these conductors experience an internal induced voltage which cause eddy currents to flow within them. These eddy currents, which are proportional to the square of the electromagnetic field strength and to the square of the ac frequency, produce losses which cause the temperature of the conductor to rise and are dissiIVII.4pated in the form of heat in the transformer. Losses due to eddy currents are further subdivided into loss due to eddy currents in the primary and secondary windings and loss due to eddy currents in components other than the windings. [2]

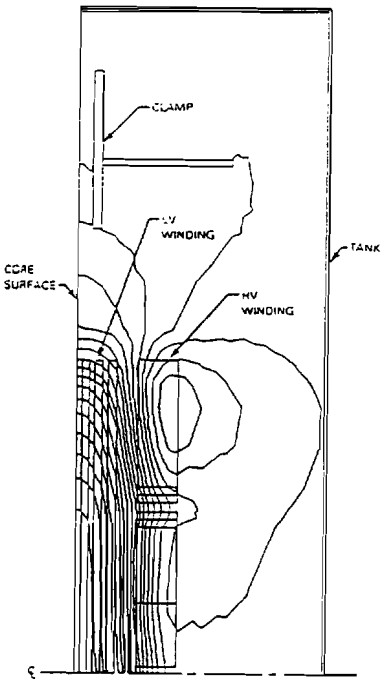

Fig. II.2-4 Electromagnetic Field Produced by Load Current in a Transformer

II.3 Causes of Distribution Transformer Losses

The cause of harmonics and distortion present in power distribution systems are caused by nonlinearities in the system, such as faults, in-rush currents, and non-linear loads imposed on the system. The widespread use of solid state controlled loads have significantly increased the amount of harmonic current in power distribution networks. Although solid state loads have been present on the distribution system for many years, their presence has become most notable over the past few years due to technological advancements in the solid state area that have produced high-power handling devices.

One such solid state device used in high-power applications is the rectifier diode. Used in a bridge rectifier configuration for single-phase applications and a six-pulse rectifier configuration for three-phase applications, the diode is a semiconductor switch which allows forward current to flow in its on state and supports a reverse voltage across its terminals in its off state. The schematic diagram for a single-phase full-wave bridge rectifier with an output filter capacitor is shown below in Fig. II.3-1. By commutation of the switch pairs, a full-wave rectified voltage is obtained at the output terminals from an ac source applied at its input terminals.

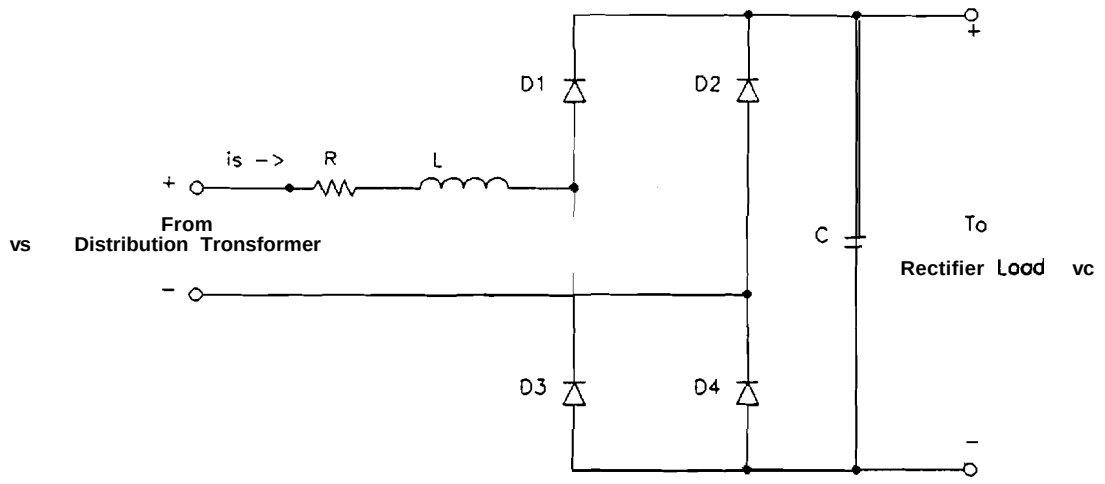

Fig. II.3-1 Single-Phase Full-Wave Bridge Rectifier with Output Filter Capacitor

Due to the large ripple content in the output voltage, a capacitor is placed across the output terminals to smooth out the dc voltage. The diode pairs of the bridge will conduct during the period of the cycle when the input voltage exceeds the voltage across the filter capacitor. This relatively short conduction period produces a current waveshape such as that shown in Fig. II.3-2. Because of its nonsinusoidal characteristic, this waveshape is rich in odd-harmonics and has a large harmonic distortion.

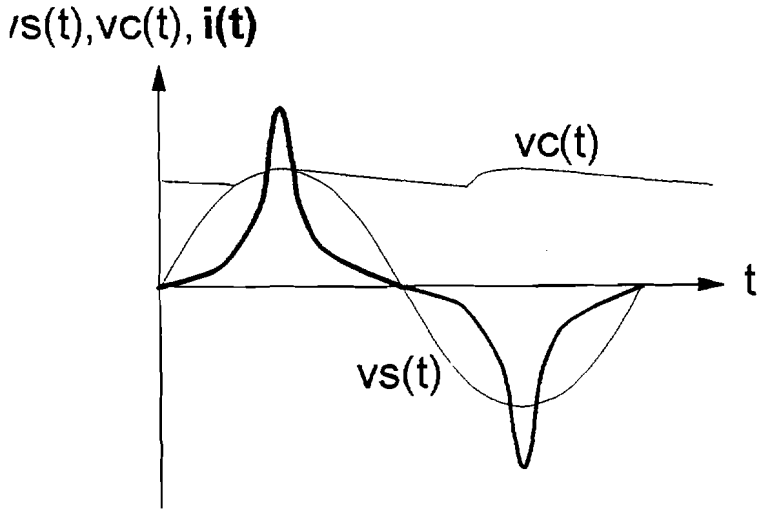

Fig. II.3-2 Voltage and Current Characteristics of Single-Phase Full-Wave Bridge Rectifier

One high-power application of the rectifier is its use in the adjustable speed drive to provide a dc input voltage for a three-phase inverter used to power a large horsepower synchronous or inductive motor. Another application of the rectifier is its use in the compact fluorescent lamp to provide a dc input voltage for a single-phase inverter used to power the lamp. Although the current consumed by a compact fluorescent lamp is relatively small in comparison to that of an adjustable speed drive, its use throughout a large building can result in a large harmonic load imposed on the distribution system.

When such loads are connected to the distribution system, the rectifier circuit is a potent source of nonsinusoidal current imposed on the secondary of the distribution transformer. Since the eddy-current loss in the winding conductors is proportional to the square of the applied ac frequency, there is a significant loss in the transformer windings due to the large harmonic content in the applied rectifier supply current.

II.4 Effects of Transformer Losses

Both no-load and load losses which are incurred in the distribution transformer are dissipated as heat. Most distribution transformers are immersed in an oil bath to improve heat conduction from the windings and core material to the transformer enclosure:. This oil bath effectively dissipates the heat incurred in the windings and core material into the atmosphere.

The heated oil of the transformer, which is in the presence of air, slowly oxidizes and forms a sludge. When this sludge adheres to the inner surfaces of the transformer, the convection of heat from the windings and core material to the enclosure is reduced. This leads to heat buildup in the windings and causes brittleness and a loss of mechanical strength in the winding insulation.

To counter the effects of winding insulation breakdown, periodic testing and filtering or replacement of the transformer oil is done. An increase in transformer losses will directly lead to an increase in maintenance costs. Thus, in most cases, an increase in transformer losses leads to a decrease of its normal economic life expectancy. [3]

II.5 Recommended Practice for Establishing Transformer Capability When Supplying Nonsinusoidal Load Currents - ANSI/IEEE C57.110-1986

This standard set forth by the American National Standards Institute (ANSI) and the Institute of Electrical and Electronics Engineers (IEEE) establishes two methods for the current derating of power transformers when connected to loads which consume nonsinusoidal currents. The standard applies to nonsinusoidal load currents which have a harmonic load factor (defined as the ratio of the effective value of all the harmonics to the effective value of the fundamental harmonic) greater than 0.05 per unit. [4,5]

As was described in Section II.2, transformer losses can be divided into no-load loss and load loss. ANSI/IEEE C57.110-1986 establishes a current derating factor for power transformers by accounting for the increased load loss due to nonsinusoidal load currents. Thus, no-load loss is not accounted for in the derating procedures.

Two methods are provided for in ANSI/IEEE C57.110-1986 for the derating of power transformers. Both methods determine the current handling capability of power transformers without the loss of normal rated life expectancy. The first method, primarily for use by transformer design engineers, requires access to detailed information on loss density distribution within the transformer windings. The less-accurate second method, primarily for use by the transformer user, requires access to certified test report data only. It is assumed in both methods that the harmonic characteristics of the load current are known. The latter method for derating a transformer will be described below.

With access to certified test report data, the following equation for the derating of a transformer may be used:

$$I\max(\text{pu}) = \left[\frac{}{1 + \left[\left(\Sigma f_h^2 h^2 / \Sigma f_h^2 \right) P\text{ec-r (pu)} \right]} \right]^{1/2}$$

where:

Imax (pu) Maximum permissible rms nonsinusoidal load current (per unit of rated rms load current)

PII-r (pu)	Load loss density under rated conditions (per unit of rated load I^2R loss density)
Pec-r (pu)	Winding eddy-current loss under rated conditions (per unit of rated load I^2R loss)
f_h	Harmonic current distribution factor for harmonic "h" (equal to the harmonic "h" component of current divided by the fundamental 60 Hz component of current for any given loading level)
h	Harmonic order

Using the above equation, it is assumed that the nonsinusoidal load current applied to the transformer has an rms magnitude of 1 per unit. It is also assumed that the per unit rms current for harmonic order "h" is terms of the rated rms load current, I_h (pu), is known. In other words, the harmonic distribution of the load current applied to the transformer is assumecl to be known.

The harmonic current distribution factor, f_h, can be determined for a specific harmonic order, h, by dividing I_h by the rms current at the fundamental frequency of 60 Hz (h=1), I_1.

The per unit eddy-current loss in the region of highest loss density defined for 60 Hz operation at rated current, Pec-r (pu), can be obtained from certified test report data for the individual transformer which is usually provided by the manufacturer. The maximum per unit local loss density under rated conditions, Pll-r (pu), can then be defined as 1 + Pec-r (pu).

The maximum permissible per unit rms nonsinusoidal load current in terms of the rated rms load current, Imax (pu), is then obtained using the equation shown above. The maximum permissible rms nonsinusoidal load current can be obtained by multiplying Imax (pu) by the rms sine wave current under rated frequency and load conditions, I_1.

It should be noted that this procedure for the derating of a transformer when supplying nonsinusoidal load currents produces a conservative derating factor. This is due to the fact that procedure produces a derated current factor for a load current applied to the transformer which is 100% nonlinear. In most practical cases, the load applied to the distribution transformer will consist of a percentage of linear load which will not contribute to excessive losses in the transformer. [5]

II.6 Conclusion

The proliferation of nonlinear loads throughout the utility distribution system has provided for much concern due to increase of distribution transformer losses. The nonsinusoidal load currents consumed by these nonlinear loads have a direct impact on the operational lifetime of the distribution transformer. Economically speaking, the use of energy-efficient solid-state loads by the consumer will be at the cost of the utility in terms of increased maintenance and oversizing of distribution transformers.

II.7 Bibliography

[1] Electric *Machinery*, Ch. 1 & 2, A.E. Fitzgerald, Charles Kingley, Jr., Stephen D. Umans, Mc-Graw Hill, Inc., New York, 1990.

[2] Apppendix to ANSI/IEEE C57.110-1986, "Tutorial Discussion of Transformer Losses and the Effect of Harmonic Currents on These Losses."

[3] *Magnetic* Circuits and *Transformers*, Ch. 5, 8, &16, MIT Electrical Engineering Staff, John Wiley & Sons, Inc., New York, 1949.

[4] ANSI/IEEE Std 519-1990, IEEE Recommended Practices and Requirements for Harmonic Control in Electrical Power Systems.

[5] ANSI/IEEE C57.110-1986, IEEE Recommended Practice for Establishing Transformer Capability When Supplying Nonsinusoidal Load Currents.

CHAPTER III
WATT-HOUR METER ERROR
Atulya Risal

III.1 Present practices on revenue metering

The demand for more efficient use of electric energy along with the increased use of solid state switches for power flow control and the renewed interest in alternative energy sources has brought power system harmonics under a closer scrutiny. In addition to degradation of power quality, the presence of harmonics on the voltage and current wave forms at the point of common coupling (PCC) has undesirable effects on the measurement of energy consumption.

Depending on classification of the loads, residential, commercial or industrial, utilities throughout the United States have different methods of assessing rates that may or may not account for the power factor and peak demand. In general customers on "demand rates" (i.e., those that pay for both energy and peak power demand) pay also "multiplier" based on their load power factor. The power factor is usually measured indirectly by measuring total active power integrated over one month (i.e. energy) W_p, and integrated vars, W_q

$$W_q = \int_{\text{Month}} Q(t)dt$$

where $Q(t)$ is the reactive power demand. Then

$$pf = \frac{W_p}{\sqrt{W_p^2 + W_q^2}}.$$

Alternatively, the complex power demand $S(t)$ may be measured over one month,

$$W_s = \int_{\text{Month}} S(t)dt$$

and

$$pf = \frac{W_p}{W_s}.$$

In either case, most present meters are not designed to measure either active or reactive power consumed at harmonic frequencies. Note also the distinction between the terms displacement power factor (DPF) and true power factor (TPF). The DPF is the cosine of the angle between the 60 Hz load current and voltage components. It is the power factor of the 60 Hz component. True power factor is

$$TPF = \frac{P}{S},$$

where P is the total active power over all frequencies- not only 60 Hz. Reference [1] contains more elaborate discussion of these terms.

The various electrical quantities mentioned above are measured with the help of either an induction disk based meters or digital electronic meters. Hence the error analysis under harmonic voltage and current distortion that is performed on the watt-hour meter can be easily extended to analyze other measurement errors.

III.2 Induction watt-hour meter

Induction watt-hour meter IWHM operation is similar to that of an induction motor. In a polyphase induction motor the stator windings are displaced in space in the same relations as the voltages are displaced in time. The resulting uniform stator flux that rotates about the rotor axis with uniform speed causes short-circuitecl rotor e.m.f and hence eddy currents. These currents react with the original flux to create a driving torque of the "motor". The single phase watt-hour meter uses an aluminum disk as the rotor and a voltage and current coil to create voltage and current fluxes that are in quadrature. This is done by making the voltage electromagnet as inductive as possible and the current electromagnet non-inductive. This produces a similar to that of two phase induction motor

[2]. The operation criteria of the watt-hour meter can be explained in terms; of two distinct parameters: the driving torque and the braking torque.

Driving torque is created through two different components. The interaction of the voltage coil flux Φ_E with the eddy currents I, caused by the change in current flux creates a torque for a load power factor $\cos(\theta)$ given by,

$$T_1 = k_1 \Phi_E I_I \cos(\theta). \qquad [III.1]$$

The second component of torque is produced through the interaction of current flux **O,** with eddy currents I, induced by the voltage flux Φ_E,

$$T_2 = k_2 \Phi_I I_E \cos(\theta). \qquad [III.2]$$

Both eddy currents are proportional to:

- thickness of the disk
- conductivity
- source frequency
- flux magnitude.

Alternatively,

$$I, \propto \Phi_I f \quad \text{and} \quad I, \propto \Phi_E f.$$

The total driving torque is then

$$T_D = T_1 + T_2 = (k_1 \Phi_E I_I + k_2 \Phi_I I_E) \cos(\theta)$$
$$= (c, \Phi_E \Phi_I f + c_2 \Phi_I \Phi_E f) \cos(\theta)$$
$$= c_3 \Phi_E \Phi_I f \cos(\theta).$$

The driving torque $T_D \propto$ EI $\cos(\theta)$ if the frequency is constant. This torque will cause the disk to rotate at an increasing speed. **A** counter mechanism or détente is required to assure that the disk rotates at a steady speed proportional to the torque.

The damping torque is mostly attributed to the permanent magnet and the electromagnet flux. The method used in induction watt hour meter to place permanent

magnets either singly or in pairs with the poles on the opposite sides of the disk. When the disk passes through the flux created by the permanent magnet, voltage and eddy currents are induced which react with the fluxes to create a braking torque

$$T_m = c_1 \Phi_m I_m, \qquad [III.3]$$

but

$$I_m = \frac{E_\Phi}{Z} = c_2 \Phi_m S \qquad [III.4]$$

so

$$T_m = c_3 \Phi_m^2 S \qquad [III.5]$$

Thus if Φ_m is constant, the permanent magnet braking torque is proportional to the speed. Although the permanent magnets are the only components placed to provide braking torque, there is other factors that provide braking. The movement of the disk through the very same flux that created the motion produces an opposing torque. Also the friction at the bearing of the rotating disk acts as a braking torque. The friction is mechanical in nature and can be compensated by appropriate design. The electromagnetic braking torque created by the current and voltage flux as with permanent magnets is proportional to the square of the flux,

$$T_E = c_4 \Phi_E^2 S \qquad [III.6]$$

$$T_I = c_5 \Phi_i^2 S. \qquad [III.7]$$

The disk speed will reach a steady state when the driving torque balances the damping torque. Since

$$T_D = K_1 * \text{Load}$$

and

$$T_B = K_2 * \text{Speed},$$

if

$$T_D = T_B$$

then

$$\text{Speed} = \frac{K_1}{K_2} * \text{Load}.$$

Therefore, the speed of the disk is proportional to the load. This calculation is based on the assumption of sinusoidal voltage and current creating sinusoidal fluxes at the fundamental frequency of interest.

Under ideal calculations, any shift in fundamental frequency does not impact the speed and hence the load measurement of the watt-hour meter. Since the current coil is virtually non-inductive, the flux created by this series coil will be independent of the frequency. The eddy currents induced in the disk however, are proportional to the rate of change of flux and hence frequency. These eddy currents react with the flux created by the voltage coil which will vary inversely with the frequency due to high induction of the coil. The driving torque created by the reaction of the voltage flux (proportional to 1/f) and the eddy current (proportional to f) will be proportional to their product and independent of frequency. The driving torque due to the interaction of current flux and voltage coil induced eddy currents is also independent of the frequency. The current flux has no frequency dependence. The voltage flux (proportional to 1/f) and the eddy current (proportional to f) due to the flux neutralize each other producing no net frequency dependence.

Although the treatment above shows the induction watt-hour meter to perform accurately under all frequencies, experience has shown that it is seldom the case. The discrepancies can be explained if we take a closer look at the meter. The effective voltage flux, assumed to be purely sinusoidal, in reality is distorted and contains higher harmonics, particularly 3rd and 5th. Also with inductive load, the losses (copper and iron) in the voltage electromagnet causes the current to deviate from being in quadrature with the voltage. The iron losses increase faster with frequency than copper losses decrease. The

increase in total loss causes the current to be lag by less than 90 degrees. At the same time the non inductive current coil starts to show inductance at higher frequencies. The principal source of registration error at higher frequencies, however, is the phase angle increase of the equivalent disk impedance. The increase in disk inductance raises the impedance of the disk with higher frequency decreasing the eddy currents and subsequently the torque. The increase in disk resistance with frequency and its effect on the watt-hour meter registration is very minimal [3]

It is to be expected that depending on design criteria, WHMs will have different frequency responses. The variation in the parameters of IWHM lead to different conclusions when tests are conducted [4]. However, a more accurate representation of IWHM can be made if we model the equipment in frequency domain. Makram et al [5] have successfully analyzed this model which overcomes various difficulties associated with time domain model such as interrelated functions and machine dependent time constants. In addition, any approach to analyze the IWHM by summing the effect of individual harmonics will give flawed results due to the non-linear nature of flux paths around saturation. Following the analysis of Makram et al, consider the distorted voltage and current written in Fourier components as,

$$v(t) = V\sin(\omega_0 t) + \sum_{k=2}^{NH_v} b_{kv} V \sin(k\omega_0 t - \delta_k) \qquad [III.8]$$

and

$$i(t) = I\sin(\omega_0 t - \theta) + \sum_{k=2}^{NH_i} b_{ki} I \sin(k\omega_0 t - \theta_k - \delta_k) \qquad [III.9]$$

Using Fourier Transform, the wave form can be represented by a magnitude and phase given by,

$$v_k(t) = V_{mk}\cos(\omega_k t + \theta_{vk}) \qquad [III.10]$$

$$i_k(t) = I_{mk}\cos(\omega_k t + \theta_{ik}) \qquad [III.11]$$

For linear magnetic circuit, the flux due to each voltage and current component at each frequency can be summed to obtain total flux,

$$\Phi_v(t) = \sum_{k=1}^{NH_v} \frac{C_v V_{mk}}{Z_{vk}} \cos(\omega_k t + \theta_{vk} - \alpha_{vk}) \qquad [III.12]$$

$$\Phi_i(t) = \sum_{k=1}^{NH_i} C_i I_{mk} \cos(\omega_k t + \theta_{ik}) \qquad [III.13]$$

where C_v, C_i are proportionality constants of the fluxes due to the voltage and current coils.

$$Z_{vk} = \sqrt{R_{vk}^2 + (\omega_k L_{vk})^2} \qquad [III.14]$$

is the magnitude and

$$\alpha_{vk} = \tan^{-1}\left(\frac{\omega_k L_{vk}}{R_{vk}}\right) \qquad [III.15]$$

is the angle of the voltage coil impedance.

The saturation effect can be modeled by using effective flux as defined by,

$$\Phi' = a_1\Phi + a_2\Phi^2 + a_3\Phi^3. \qquad [III.16]$$

for both Φ_v and Φ_i.

Then by applying Fourier Transform to the time domain effective flux, phasor representation can be expressed as,

$$\left|\Phi_v'\right| = \left(\frac{C_v V_{mk}'}{Z_{vk}}\right), \quad \arg\left(\Phi_v'\right) = (\theta_{vk}' - \alpha_{vk}) \qquad [III.17]$$

and

$$\left|\Phi_i'\right| = C_i I_{mk}', \quad \arg\left(\Phi_i'\right) = (\theta_{ik}'). \qquad [III.18]$$

The primed variables are the equivalent terms after taking non-linearity of the magnetic circuit in to account. The emf induced on the disk by the effective fluxes can be represented at each individual frequency as,

$$i_{dv} = \left(\frac{C_v V_{mk}''}{Z_{dk}}\right)\omega_k \sin(\omega_k t + \theta_{vk}' - \alpha_{vk} - \alpha_{dk}) \qquad [III.19]$$

and

$$i_{di} = \left(\frac{C_i I_{mk}}{Z_{dk}} \right) \omega_k \sin(\omega_k t + \theta'_{ik} - \alpha_{dk}). \qquad \text{[III.20]}$$

Where Z_{dk} and $a_{,,}$ are the magnitude and the angle of the disk impedance and

$$V''_{mk} = \frac{V_{mk}}{Z_{vk}} \qquad k = 1,2,3\ldots\ldots, NH_v.$$

Thus the driving torque defined by,

$$\tau_d = \frac{1}{T} \int_0^T [\Phi_v(t) i_{di}(t) - \Phi_i(t) i_{dv}(t)] dt \qquad \text{[III.21]}$$

becomes

$$\tau_{dk} = \sum_{k=1}^{NH} \frac{1}{T} \int_0^T [C_i C_v V''_{mk} \cos(\omega_k t + \theta'_{vk} - \alpha_{vk}) \frac{\omega_k I'_{mk} \sin(\omega_k t + \theta'_{ik} - \alpha_{dk})}{R_{dk} \sqrt{1 + \left(\frac{\omega_k L_{dk}}{R_{dk}} \right)^2}} -$$

$$C_i C_v I'_{mk} \cos(\omega_k t + \theta'_{ik}) \frac{\omega_k V''_{mk} \sin(\omega_k t + \theta'_{vk} - \alpha_{vk} - \alpha_{dk})}{R_{dk} \sqrt{1 + \left(\frac{\omega_k L_{dk}}{R_{dk}} \right)^2}}] \, dt.$$

[III.22]

Following equation 111.21, under idealized conditions of frequency independence and linear magnetic circuit, the ideal driving torque of a IWHM can be expressed as,

$$\tau_{Idk} = \sum_{k=1}^{NH} \frac{\omega_k C_I C_v I_{mk} V_{mk}}{R_{dk}} \sin(\theta_{vk} + 0, + a_{,,,}). \qquad \text{[III.23]}$$

The registration error E based on ideal and modified torque equations becomes,

$$\%E = \left[\frac{(\tau_{dk} - \tau_{Idk})}{\tau_{Idk}} \right] * 100. \qquad \text{[III.24]}$$

Figure III.1 shows the plots of %E under various conditions and selected values of the non-linear model coefficients.

Fig. III.1 Registration Error [6]

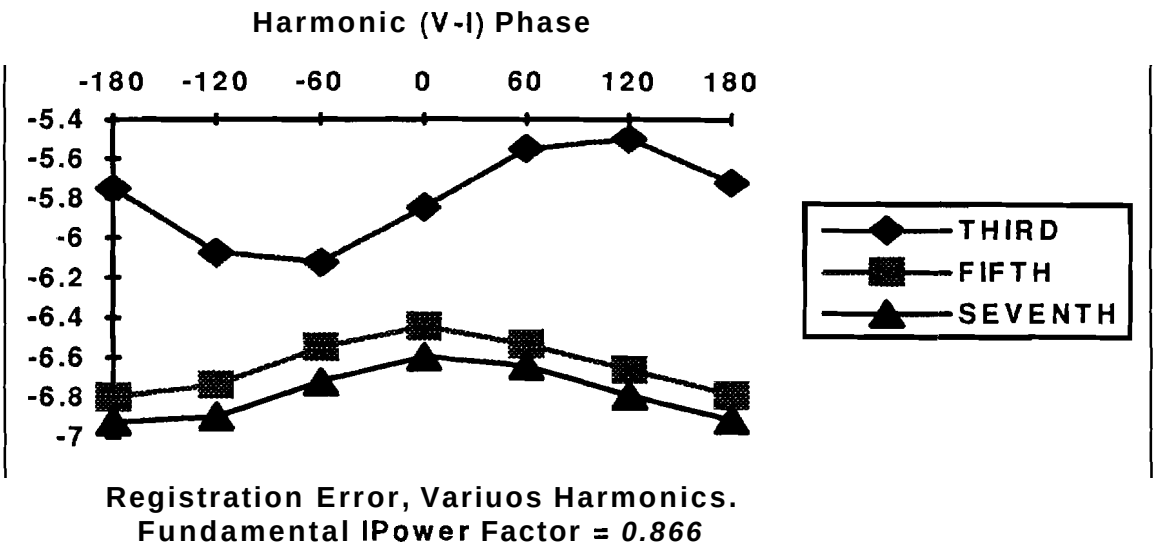

Registration Error, Variuos Harmonics.
Fundamental IPower Factor = *0.866*

It should be noted that the characteristics shown in the figures are not universal. Specifically, the choice of design parameters will yield different error curves. Also, the phase angle of voltage and current harmonics have a significant impact in the sign and magnitude of error. Table 1 [7] shows the effect of varying firing angles on a different IWHM. Furthermore, this model does not incorporate the braking torque due to the movement of disk through the flux. This torque is also dependent on frequency. Under appropriate considerations, the errors should be lower.

TABLE III.1
% METER ERRORS FOR RATED VOLTAGE AND CURRENT FUNDAMENTALS AT DIFFERENT FIRING ANGLES a [7]

	Six - Pulse	Rectifier	Rectifier Load	Supplied With Back	Non-Linear emf
a	YY or M	YA or AY	1- Phase	1- Phase*	3-Phase
0	0.82	0.31	-1.11	-1.79	-0.81
1	0.51	0.42	-0.71	-0.89	0.01
π/6	0.17	0.59	0.03	0.29	0.97
π/4	0.25	0.67	1.21	1.74	1.57
π/3	0.52	0.19	2.32	3.07	1.93

* 1% of 3rd harmonic voltage is added in phase with the fundamental phase

In conclusion, although various authors have tested the IWHM under distorted wave forms, the results are seldom similar. With the various component parameters available for the designer, the inconsistency is readily explained. The frequency model is an attempt to universalize the design and analysis of IWHM for performance under harmonic voltage and currents. The calculated error curves indicate that IWHM under-register the energy consumed. When the IWHM is analyzed, it can be said that harmonics in power system is not only impacting power quality but revenue as well

III.3 Electronic revenue meters

Electronic meters are based on digital conversion of voltage and current measurements. The digital output is directly related to the product of the two quantities. There are various mathematical techniques that can be applied to convert analog measurements into power and energy readings. The simplest of the ideas involves multiplying the current and voltage measurements, converting the analog power to frequency and using a pulse counter to reflect output. Bohesian et al suggest a method where the current and voltage signals are used to generate two dc signals the which are translated into energy reading [8]. Another procedure samples the voltage and current magnitude periodically at frequencies much higher than the supply frequency and manipulates the two numbers to obtain active reactive and other power readings [9]. There are various well established algorithms that can be used to indicate the energy measurements from the digital samples. Present electronic meters in use mostly employ pulse width modulation (PWM) technique.

In PWM, one of the current/voltage signal defines the magnitude: of a pulse train while the other signal determines the interval. Following figure 111.2, if we let U_x be one of the inputs and let U_y be the other, then with,

$$\frac{T_1}{T_0} = k_1 U_x \qquad \text{[III.25]}$$

and

$$U_m(t) = \begin{cases} U_y & \text{for } t_i < t \le t_i + T_1 \\ 0 & \text{for } t_i + T, < t \le t_i + T_0 = t_{i+1} \end{cases}, \qquad \text{[III.26]}$$

The average value of the pulse train is proportional to the product of the input quantities

$$k_2 \overline{U}_m = k_2 U_y \frac{T_1}{T_0} = k_1 k_2 U_y U_x. \qquad [III.27]$$

which reflects the power level [10].

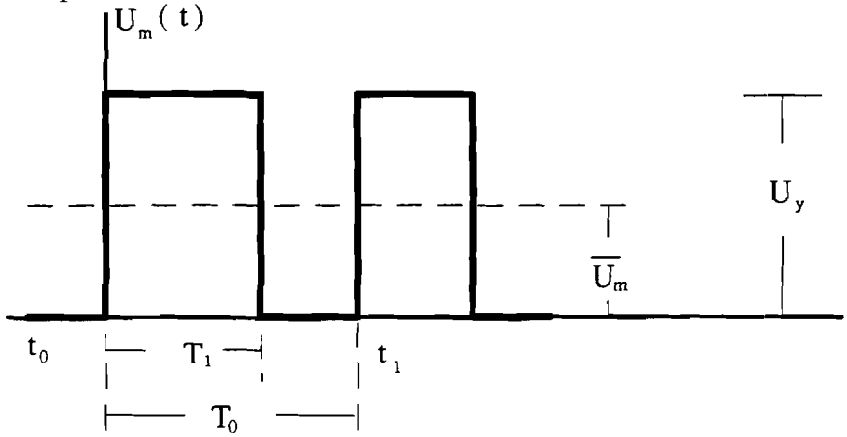

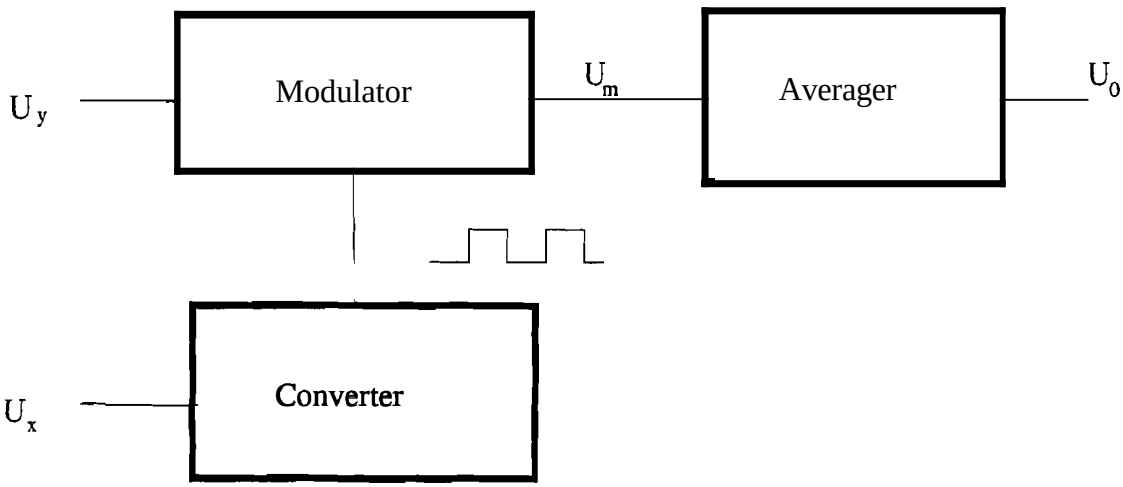

Fig. III.2 Pulse Width Modulation

Another set of electronic meters implement the transconductance method to measure the power and hence energy. In this method (figure III.3), the current in the line is measured by the voltage developed across a shunt and the line voltage is measured by using a voltage divider. The shunt voltage and the potentiometer voltages are multiplied

electronically and a pulse train of frequency proportional to the product is generated and accumulated to indicate power consumption [11].

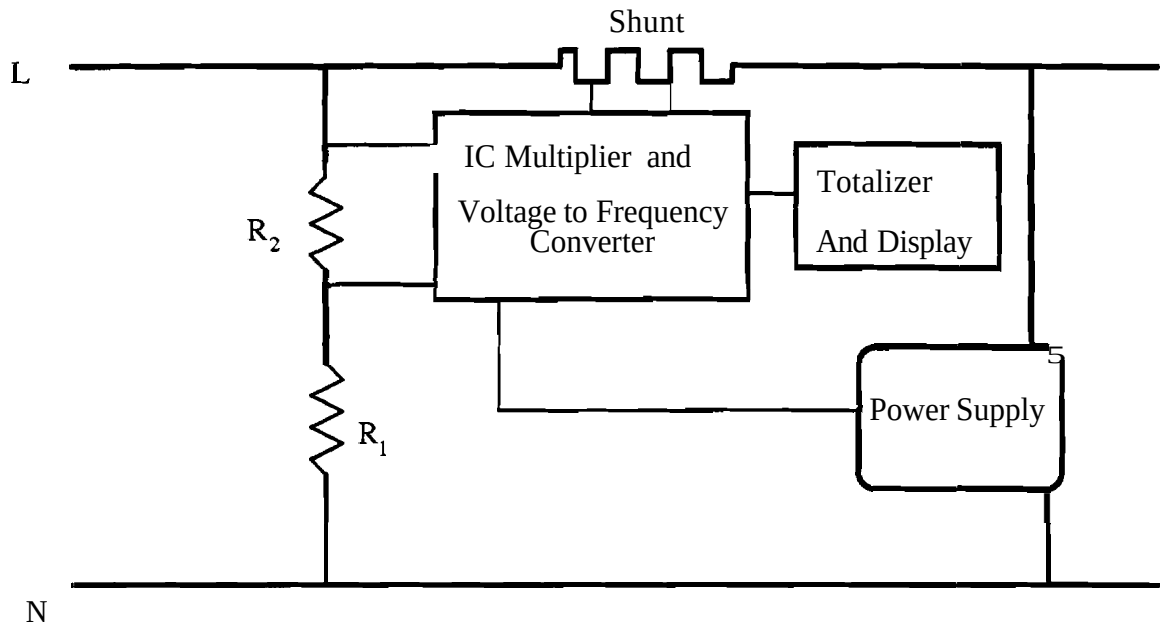

Fig. III.3. Transconductance Energy Measurement

As in the analog case, if we decompose the current and voltage wave forms into their harmonic components [12],

$$V = V_0 + \sum_{h=1}^{NH_v} V_h \sin(h\omega_0 + \phi_{vh}). \qquad [III.28]$$

$$I = I_0 + \sum_{h=1}^{NH_h} I_h \sin(h\omega_0 + \phi_{Ih}). \qquad [III.29]$$

The power spectrum obtained by multiplying the two terms is of the form.

$$P = P_0 + \sum_{h=1}^{2NH} P_h \sin(h\omega_0 + \phi_{Pn}) \qquad [III.30]$$

The summed term averages to zero for a full cycle and the only term that contributes to the energy measurement is,

$$P_0 = V_0 I_0 + \sum_{h=1}^{NH} \frac{V_h I_h}{2} \cos(\phi_{vh} - \phi_{Ih}). \qquad [III.31]$$

Only current and voltage components of the same frequency contribute to the energy consumed. In digital measurement of regular interval sampling, theory dictates that frequency components above $f_s / 2$ (where f_s is the sampling frequency) cannot be resolved. This leads to the effect known as aliasing where the frequency component above: $f_s / 2$ appear between DC and $f_s / 2$ and although the original wave form cannot be reconstructed, the average energy can still be recorded. However, the accuracy will be affected if,

- higher frequency components are aliased to DC,
- frequency components are aliased to top of other frequency component producing interference,
- signal is not in steady state.

Table III.2 shows the results of error measurement performed on a class 2 sampling electronic polyphase meter under different voltage and current distortion [13].

Table 111.2.
Class 2 sampling watt-hour meter error under various conditions. Fundamental power factor = 1. Worst case values selected. [13]

Test	Voltage	Current	%Error (Wh)
1	Fundamental Only	Fundamental Plus 10% 3rd Harmonic	-0.14
2	Fundamental Only	Half Wave Rectified	+0.88
3	Fund + 5% 3rd + 6% 5th + 5% 7th + 1.5% 9th 3.5% 11th 3% 13th.	Fundamental Plus Harmonics proportional to voltage	+0.1
4	Fundamental Only	Phase Fired at 90 and 270 Degrees.	+0.46

By carefully selecting the sampling method and frequency, much of the errors in energy measurement can be reduced to a negligible quantity. If the sampling frequency is chosen to be asynchronous with all harmonics, the DC aliasing can be avoided. Similarly, by introducing a third or fourth order low-pass filter prior to detection, sampling frequency can be chosen such that none of the band limited harmonics can interfere with each other. Some form of low-pass filtering is necessary to avoid RF and transient interference as well. At first glance, the sample-and-hold in analog to digital conversion should also produce error measurement that is dependent on the interpolation method used to reconstruct the signal. This however is not the case since the error depends on the position of the wave form and with the sampling frequency not related to the main frequency, the sign of the error varies. This variation will eventually cancel out provided that the approximation method is not biased towards any error direction.. The time required for this zero averaging is of course dependent on the magnitude of harmonic distortion [14].

With the rapid growth in the integrated circuit manufacturing technology, it is now possible to incorporate multitude of functions into an electronic meter with the use of microprocessors and memories. The same measurement principles utilized for watt-hour measurement can be extended to obtain VAR, peak demand and other quantities. The errors in these quantities are subject to similar conditions.

III.4 Conclusion

The effects of higher power rated electronically controlled loacls are not only confined to power quality but revenue as well. It has been shown in this paper that both the induction watt-hour meter and solid state meter registrations show error when subjected to distorted voltage and current wave forms. It is clear that the question of who is paying for the harmonic power cannot be answered in an universal basis, the design of each meter (both analog and digital) can make the registration error either positive or negative. Furthermore, the load conditions and the phase angle of the harmonic current and voltage play a significant role in meter registration. Although designed for power consumption measurement at fundamental frequency only, the induction watt-hour meter has proved resilient enough to withstand harmonic distortions to some extent. If designed appropriately, the electronic meters definitely have the advantage of being able to record power consumption at higher harmonics. With the solid state combination meters rapidly replacing the analog counterparts, more attention would have, to be paid to the frequency characteristics of the electronic meters to obtain a more universal model. Thus enabling the utilities to make appropriate adjustments to rate structures under non-sinusoidal power consumption.

References.

[1] W. Sheperd, P. Zand, Energy Flow And Power Factor In Nonsinusoidal Circuits, Cambridge University Press, Cambridge, 1979.

[2] A. E. Knowlton, Electric Power Metering, McGraw-Hill Book Company, New York, 1934.

[3] Y. Baghouz, O. T. Tan, "Harmonic Analysis of Induction Watthour Meter Performance", IEEE Transactions on Power Apparatus and Systems, Vol. PAS-104, No. 2, February 1985. pp 399-406.

[4] A. J. Baggot, "The Effect of Waveshape Distortions on the Measurement of Energy Tarrif Meters," IEE Conference Publication, No.156, November, 1977. pp 280-284

[5] E. B. Makram, C. L. Wright, A.A. Girgis, "A Harmonic Analysis of the Induction Watthour Meter's Registration Error," IEEE Transactions on Power Delivery, Vol. 7, No. 3, July, 1992. pp 1080-88.

[6] ibid.

[7] [3].

[8] D. Boghesian, M.A.H. Abdul-Karim, "A Novel Electronic Energy Meter," IEE Conference Publication, No.156, November, 1977. pp 252-255.

[9] G. W. Swift, "Current and Voltage Waveform Sampling Methods for Digital Protection and Metering Devices," IEEE Industry Application Society Annual Meeting, October, 1987. pp 1347-1351.

[10] B. M. Stojanovic, P. M. Bosnjakovic, J. R. Kucina, " New Wattmeter Base Opto-Coupler," IEE Conference Publication, No.156, November, 1977. pp 261-263.

[11] A. J. Ley, "The Solid State Domestic Watthour Meter, " IEE Conference Publication, No.217, October, 1982. pp 9-13

[12] P. R. Hutt, J. Moyce, M. Prosser, S. Day, "Intelligent Muli-Function Meters," IEE Conference Publication, No.277, **April,** 1987. pp 242-246.

[13] *G.* Lester, F. M. Gray, "The Effect of Distorted Waveforms; on a Class 2 Sampling Electronic Polyphase Meter," IEE Conference Publication, No.317, April, 1990. pp 76-79.

[14] [12]

CHAPTER IV
ARC FURNACE AND THEIR EFFECTS ON ELECTRIC POWER QUALITY

LING CHUNG

IV.l Introduction

Arc furnace is a modern technology that makes use of electrical energy on metals melting and refining metals. It has traditionally been viewed as a "dirty" load by power supply authorities. The randomly fluctuation currents drawn by the furnace can cause disturbance in voltage of the power supply system. These can results in annoying lamp flicker, particularly when the fluctuations contain frequency components in the 6 to 14 Hz range since human eyes are very sensitive in this range.

Traditionally the effects of the electric arc furnace on power supply system have been kept within acceptable limits by either supplying the furnace from a high capacity point in power supply or by installing reactive power compensation device. These methods are relatively expensive. A low cost alternate way is discussed in Section 5 which is using direct feedback control on flicker, with a flickermeter as the feedback transducer and the furnace transformer tap changer as the control actuator.

Section 2 reviews some general characteristics of arc furnace that includes AC and DC type of the furnace and the source of fluctuations in the system. Section 3 describes the space limitation of charge particles and the Child-Langmuir's Law, the stages of operation and the furnace operating point on an apparent power plane. Section 4 and Section 5 describe flicker

measurement and the control of flicker levels respectively. Section *6* covers the conclusion reached.

IV.2 General Characteristics of Arc Furnace

Three phases **AC** arc furnaces are commonly used by the steel making industry due to their simplicity and relative low capital price. Figure IV.1 shows a three-phase **AC** furnace configuration. The capacitors on the high side are used for filtering and power factor correction. There is a control device on the low side to control the high density graphite electrode positions to reignite extinguished arc furnace during operation. The conflict of delta connection and neutral connection may be resolved by using a ground delta. There also have filters on the high side to limit the harmonic impact of the furnace especially the third, fifth and seventh harmonics. The harmonic impact and control in power system are discussed in Chapter I.

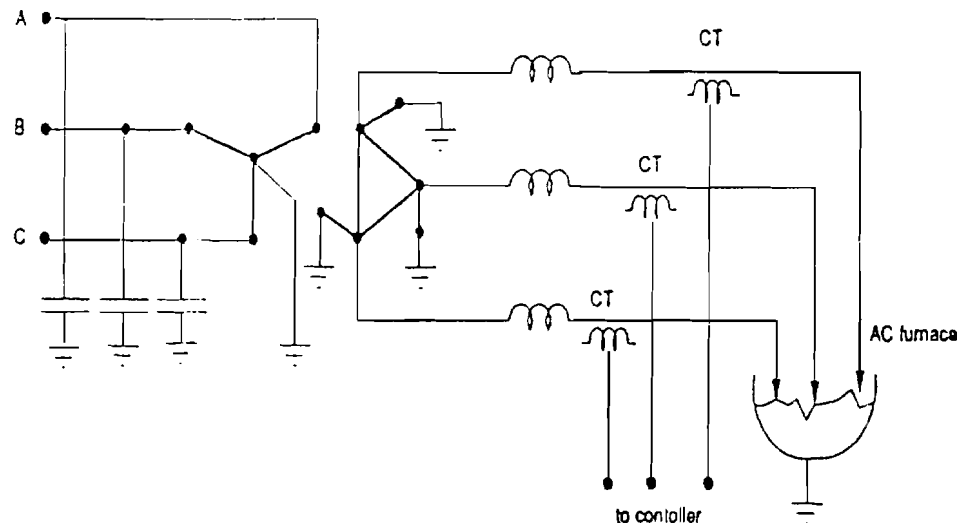

Figure IV.1 Three phase **AC** furnace configuration [1]

Figure IV.2 shows a DC furnace configuration. Although it has an overall higher cost due to the price of high power semiconductors and AC line filters, it has a higher efficiency and better control characteristics. In the electrode circuits, direct measurement of the electrode voltage and Hall effects' devices are used to sense the currents are used. These signals are then used for electrode positioning control and as the gate signals in the forced cornmutated rectifier supply. The rectifier supply may be six or twelve pulse units and the later favors for high power furnace. Harmonics filtering is more effective since harmonics in DC furnaces are concentrated at $(6n\pm1)\omega_o$, $n=0,1,2\ldots$. However, there still will be frequency components in the supply at frequencies below the supply power frequency, and at non-integral multiples of the power frequency due to the random nature of the arc.

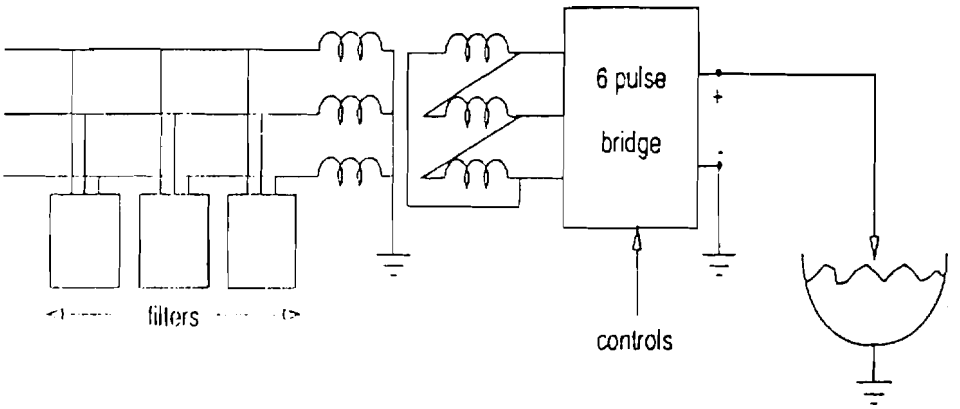

Figure IV.2 DC furnace configuration [1]

An electric arc is an electrical discharge in a gas. It is characterized by a low voltage, high current and the relationship between voltage and current are non-linear. The non-linear relationship between the voltage and current causes the harmonics to the power supply system and the random change of the arc path usually leads fluctuations in the power supply system. These fluctuations in current and voltage have their largest magnitude during the initial few minutes of the melting of the scrap. The main reasons for this are:

1. The furnace atmosphere near the electrode tip is relatively older and less easily ionized during the initial period than it is later in the melting and refining cycle.

2. Arcs intermittently fail to reignite. The electrode height regulator then lowers the electrode until the arc does reignite and this results in frequent single phasing and shorting of one electrode.

3. Changing shapes and random movements of the scraps during the beginning of melting.

4. Interaction among the three arcs (AC only) due to the associated electromagnetic forces.

IV.3 Space charge limitations and furnace operating points

When plenty of electrons are available from the cathode, the negative charge of the electron cloud near the cathode tends to repel electrons just leaving the cathode, thus limiting the attainable current density. If electrons leave the cathode with negligible kinetic energies, and ignoring the effects of

positive ions, the maximum attainable current density can be estimated from the energy conservation equation and the Poisson equation :

$$\frac{1}{2}m_e v_e^2 = e\phi(x) \qquad \text{IV-1}$$

$$\frac{d^2\phi}{dx^2} = -\frac{n_e e}{\varepsilon_o} = \frac{J}{v_e \varepsilon_o} \qquad \text{IV-2}$$

Where v_e is the electron velocity, $\phi(x)$ is the potential difference from cathode. If L is the electrode spacing and ϕ_t is the voltage difference between the them, it can be found by using the above two equations that the arc current density is

$$J = \frac{4\varepsilon_o}{9L^2}\sqrt{\frac{2e}{m_e}}\,\phi_t^{\frac{3}{2}} \propto \frac{\phi_t^{\frac{3}{2}}}{L^2} \qquad \text{IV-3}$$

This is called the "Child-Langmuir Law" [2] and can be used to predict the electrode positions and the applied voltage during the initial operating stage of arc furnace. As the scraps melting down, the increasing of ionized gas around the arc will change equation IV-3. However, there is an azimuthal magnetic field around the current path, $B_\theta = \mu_o I/2\pi r$ that induces a radially inward force, $\mathbf{J}\times\mathbf{B}_\theta$ and help to stabilize the arc.

There are many limits of arc furnace operation. The first one is arc stability. To keep the arc ignite, there must be a sufficient large voltage between the electrode and the scrap. If operation of the furnace with a long arc, low current and high power factor is attempted, eventually a point is reached at which the arcs will not reignite. This is an arc stability limit and occurs at a power factor around 0.85. Because of the relatively colder and less easily ionized condition of gases around the electrode tips during the initial melting stage, the limit of arc stability occurs at high current and low power factor. When the electrodes are in contact with the scrap, the power factor can

be as low as 0.15. It is usual to set the lower limit on power factor to 0.6 to achieve a reasonable good efficiency of the furnace.

The furnace transformer MVA rating also is a limit. Figure IV.3 shows the boundary of these limits on an apparent power plane. The shadow part is the normal operating region of an arc furnace device. During the initial melting period, the operating points are at the lower power factor and high current region. Later on, as the scrap has been melted, the operating points are at the upper left corner of the region so that a highest efficiency is attained.

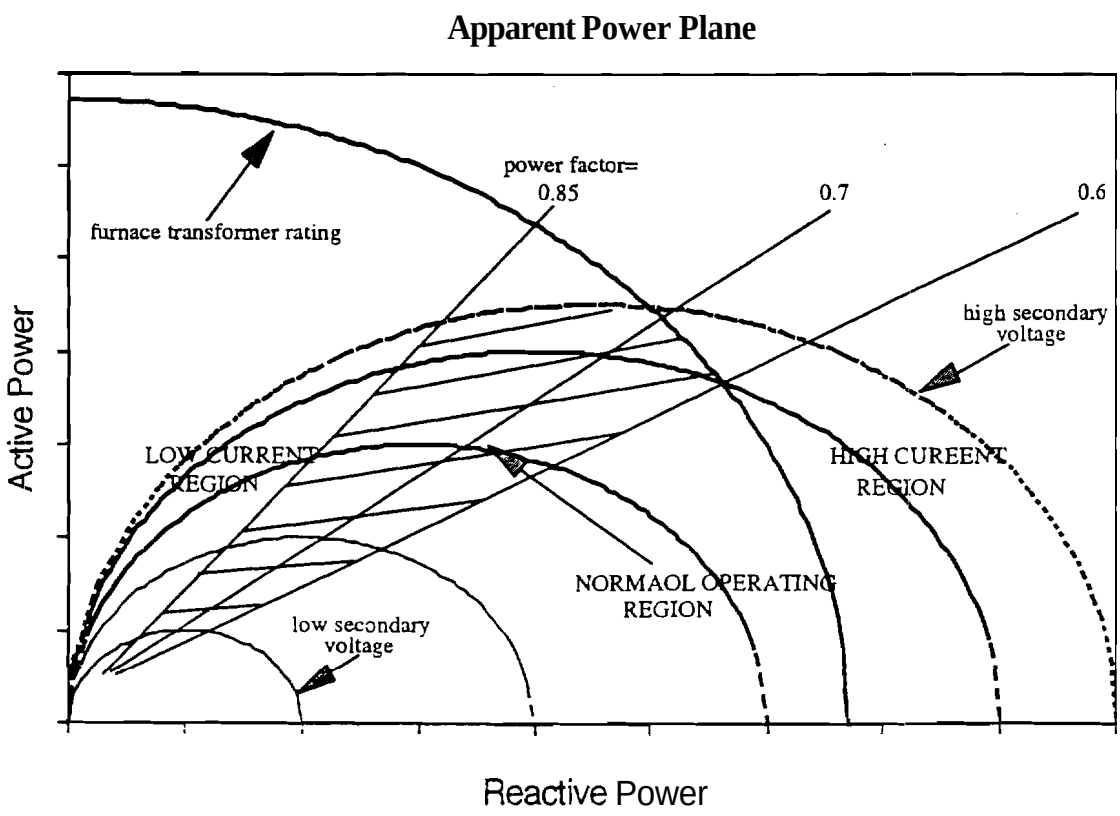

Figure IV.3 Arc furnace operating points [3]

Figure IV.4 shows the input power versus time plot for a typical melting cycle of an arc furnace. The cycle is typically of 100 rninutes duration with two scrap charges. The period of initial low power factor operation is only about three minutes per scrap charges. Most of the fluctuations are induced during the three minutes.

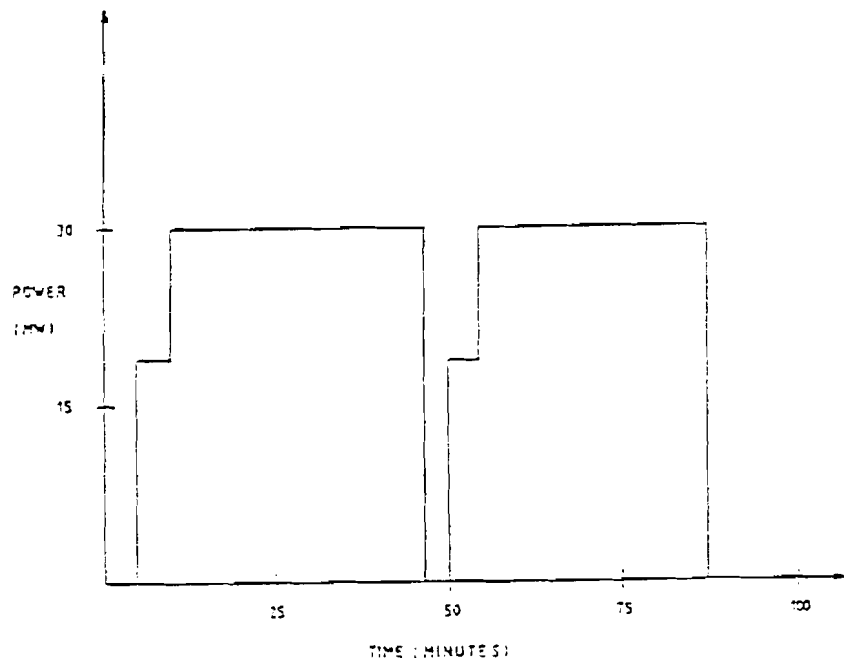

Figure IV.4 Typical melt cycle

IV.4 Flicker Measurement

The flicker level is usually measured by Short Circuit Voltage Depression Ratio, SCVD. From Figure IV.5, the SCVD can be defined as:

$$\frac{\Delta V_s}{V_o} = \frac{X_s}{X_s + X_t + X_f + X_c} \qquad \text{IV.4}$$

or

$$\frac{\Delta V_s}{V_o} = \frac{S_{scf}}{Sf,} \qquad \text{IV.5}$$

Where S_{scf} and S_{sc} are the short circuit power and system fault level power respectively. For instance, the maximum SCVD for a 36 MVA furnace operation on top tap based on a 50 MVA furnace short circuit level and a 3000 MVA system fault level can be calculated to be 1.67%.

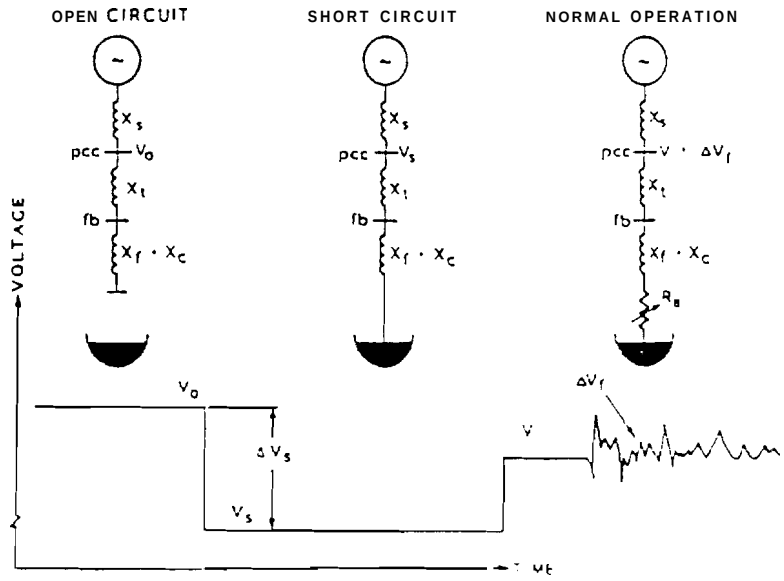

Figure IV.5 Voltage change due to operating state of an arc furnace [4]

There is not general agreement in the world on the limit of flicker levels. Many countries simply set their own limits. In Britain, the SCVD limit is 1.6% and it is 1.8% in Sweden.

The International Union for Electroheat (UIE) and the International Electrotechnical Commission (EIC) have developed a flickermeter that simulates the response of the lamp-eye-brain chain of a standard man to voltage fluctuation and produces a number of outputs which can now include a quantity called short term flicker severity, Pst. Pst is by definition based on a ten minute observation period. It measures the lamp flicker level. It is expected that Pst will gain international recognition and support.

It is found that the maximum values of Pst and SCVD are in the relationship of: Pst = SCVD/1.40. For the previous example, the maximum Pst will be 1.6711.4 = 1.2. It is recommended to set the Pst limit to 1.0 for normal operation and Pst value should not access 1.2 for maximum tolerance.

IV.5 Flicker Control

There are many ways to solve the flicker problem. Installation of compensator using large variable capacitors is commonly used. These are the static var compensators (SVC) or static watt compensators (SWC). However, the costs of these devices are high. Because flicker is strongly related to the furnace short circuit level and can be reduced if a lower furnace transformer tap is selected, a cheaper alternate way to control the flicker level is limiting the furnace transformer secondary voltage. Moreover, current variations are also smaller at lower taps.

An automatic flicker control system is shown in Figure IV.6. The system consists an UIE/IEC flickermeter, some modems and a tap changer device. Typically, there are 19 taps with voltage variation from 230 to 520 volts. The signal response time of the electronic control system is about 80 millisecond and it 5.0 second to change one tap mechanically. Usually, the minimum dwell time on each tap is 0.5 second.

The flickermeter generates a one minute P value that basically is same as Pst value but with the time period of one minutes. The P data is then transfer to the tap control device through modems. It is shown that there is a mathematical correlation between the incremental flicker levels and changes in transformer tap settings during furnace operation following scrap charging.

This helps us in designing a more efficient control algorithm. **A** typical furnace transformer tap changing rules are list in Table IV.l. This method had been used by some furnace plant in Australia and it did can control the Pst value under 1.0.

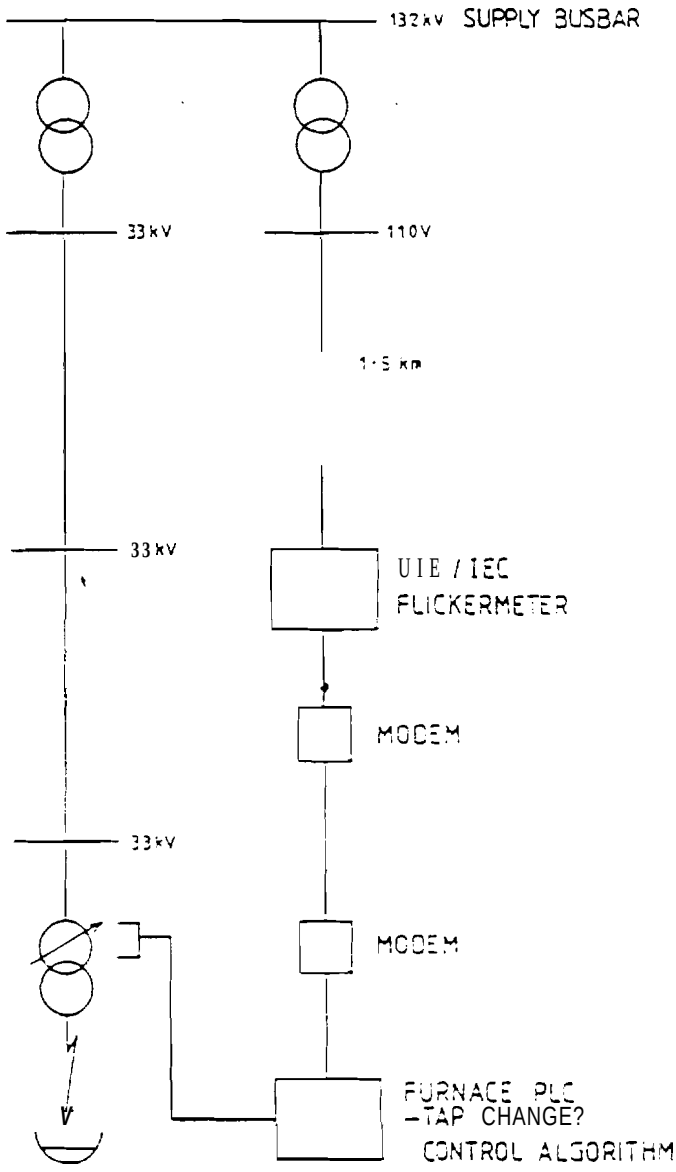

Figure IV.6 Flicker control block dia,gram

Table IV.1

Furnace transformer tap changing rules

One minute P	< 0.95		: No change
0.95	≤ One minute P	< 1.05	: Step down 1 tap
1.05	≤ One minute P	< 1.15	: Step down 2 taps
One minute P	≥ 1.15		: Step down 4 taps

IV.6 Conclusions

Arc furnace requires special attention from the power supply companies not only because it generates harmonics but also it produces random voltage fluctuation to the power system. The following relevant points are made in this chapter:

1. There is an operating region for an arc furnace. A furnace operator could reference the points in the region to achieve the best furnace efficiency.

2. Power factors can be used to adjust the operating voltage and current and to maintain the arc.

3. Voltage fluctuation in an arc furnace operation is most serious during the first three minutes. During the later operating period, since the charged scraps are melted and more ionized gas is around the arc path, the arcs become more and more stable.

4. The induced JxB inward force by the space current has a positive contribution to the arc stability especially when there presents of ionized particles

5. The calculated short circuit voltage depression ratio (SCVD) can be used to predict an uncompensated furnace system and during the period of operation, the short term flicker severity (Pst) and the SCVD are in the relationship of:

$$\text{Max. Pst} = \text{Max. SCVD}/1.4$$

6. Flicker level can be successfully controlled by adjusting the voltage of a furnace transformer on the secondary side.

IV.7 References

1. G. T. Heydt, Electric Power Quality, Stars in a Circle Publication, C1991.

2. T. J. Dolan, Fusion Research, Ch. 6, Vol. I, Pergamon Press., 1982

3. E. J. Reynolds & T. J. Watt, Control of Flicker Caused by an Electric Arc Steelmaking Furnace, Journal of Electrical and Electronics Engineering, Australia - IE Aust. & IREE Aust., Vol. 11, No. 2, June 1991.

4. G. Manchur & C. C. Erven, Development of A Model for Predicting Flicker from Electric Arc Furnace, IEEE Transactions on Power Delivery, Vol. 7, No. 1, Jan., 1992.

5. G. T. Heydt, Computer Analysis Methods for Power Systems, New York: Macmillan Publishing Company, 1986.

6. Central Station Engineers of Wesinghouse Electric Corporation, Electic Transmission and Distribution Reference Book, East Pittsburgh, Pennsylvania.

7. J. Arrillaga, D. A. Bradley, P. S. Bodger, Power System Harmonics, Chichester (West Sussex); New York: Wiley, c1985

Chapter V
Adjustable Speed Induction Motor Drives and the Impact on the Power System

Jinyu Yang

V.1 Introduction

One of the most important applications of power electronics is the control of rotating machine. Many users find that the adjustable speed drives provide higher efficiencies, better speed control, and more maintenance-free operation than other conventional drives. This encourages wider application of these drives for both ac and dc, high and low ranges of moter ratings.

Even though ASDs have many advantages such as improve system efficiency and equipment reliability, enhance product quality and reduce product waste, reduce the noise level, and save space, however, these newer technologies may have detrimental effects on the quality of the AC system. Because of the non-linearity inherent in the semiconduct devices used in electronic motor drives, they require current from the power system that is nonsinusoidal, that means the ASD acts as a generator of harmonic currents. These harmonic currents develop harmonic voltage drops across the network source impedance, causing distortion of supply voltage delivered to the ASD itself and to the other consumers in the area, and produce a harmonic resonance condition to power system.

In this paper, several control circuits for adjustable speed induction motor drives willbe introduced, at the same time, the harmonic effect to the power system and the way to absorb the harmonics wi ll be discussed.

V.2 Control Methods of Induction Motors and the Circuit Configurations

The induction motors have a number of advantages: they are lightweight, inexpensive, and low maintenance compared to dc motors. They require control of frequency, voltage, and current for variable-speed application. The power converters, inverters and ac voltage controllers can control the frequency, voltage and current to meet the drive requirements. From the knowledge of induction motors, we know that the speed and torque induction motors can be varied by one

of the following methods:

1. Stator voltage control
2. Rotor voltage control
3. Stator voltage and frequency control
4. Stator current control

1). Stator Voltage Control

From the torque equation,

$$T_d = \frac{3R_r V_s^2}{sw_s\left[\left(R_s + \frac{R_r}{s}\right)^2 + (X_s + X_r)^2\right]}$$

where V_s stator supply voltage, V;

R_r rotor resistance, Ω;

s slip;

ω_s synchorous speed, rad/sec;

R_s stator resistance, Ω;

X_s stator reactance, Ω;

X_r rotor reactance, Ω;

we know the torque is proportional to the square of the stator supply voltage: and.a reduction in stator voltage will produce a reduction in speed. Figure V.1.[2] shows the typical torque-speed characteristics for variable stator voltage.

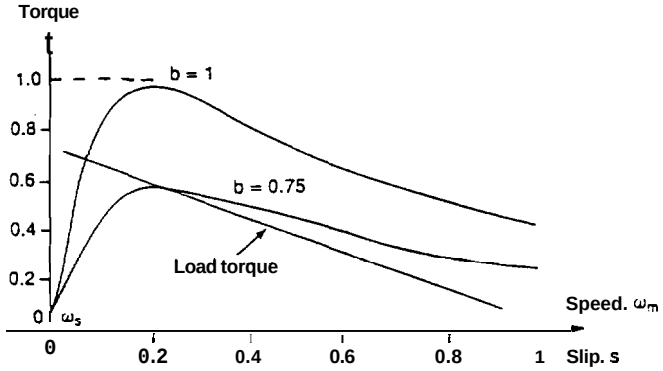

Figure V.1 Torque-speed characteristics by stator voltage control

The stator voltage can be varied by three-phase (1) ac voltage controlers, (Fig.V.2.a [1]) (2) voltage-fed variable dc link inverters, or (3) PWM inverter. (Fig.V.2.b [3])

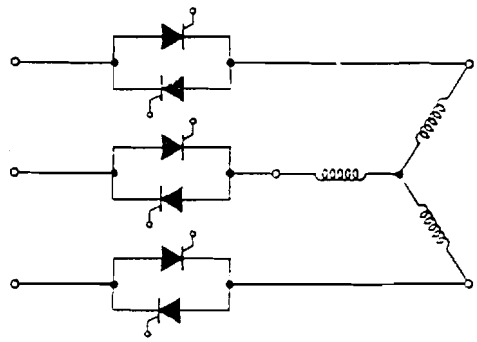

Figure V 2 a Basic stator voltage control using ac voltage controller

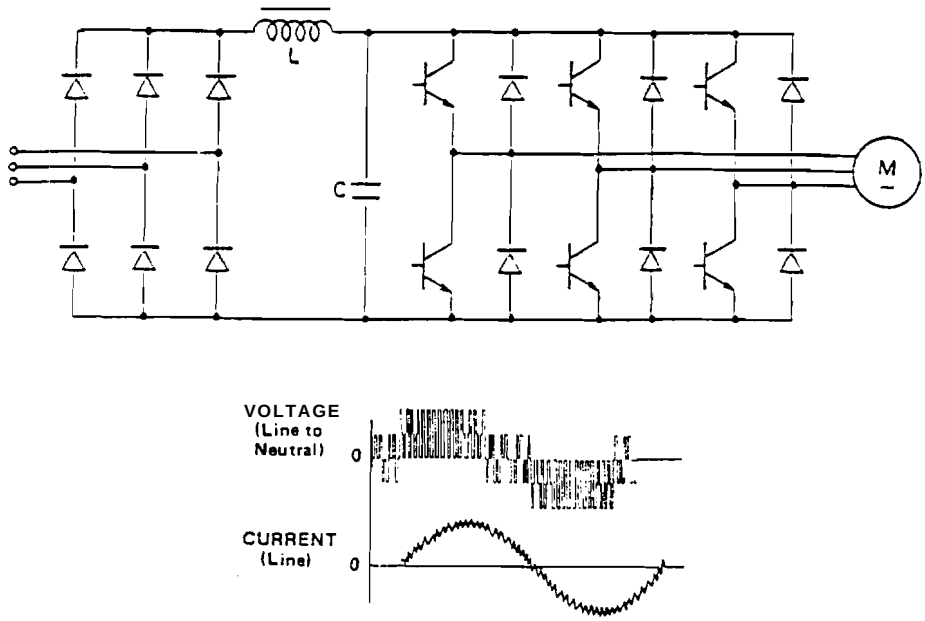

Figure V.2.b PWM inverter drive

In the fig.V.2.b, the dc voltage remains constant and PWM techniques are applied to vary the voltage within the inverter. Due to the dide rectifier, regeneration is not possible and the inverter would generate harmonics into the ac supply.

2).Rotor Voltage Control

In a wound-rotor motor, if we vary the external three-phase resistor which is connected to its slip rings, we can control the torque and speed, because the torque is proporational to the rotor resistor. The typical torque-speed characteristics for variations in rotor resistance are shown in Fig.V.3[2]

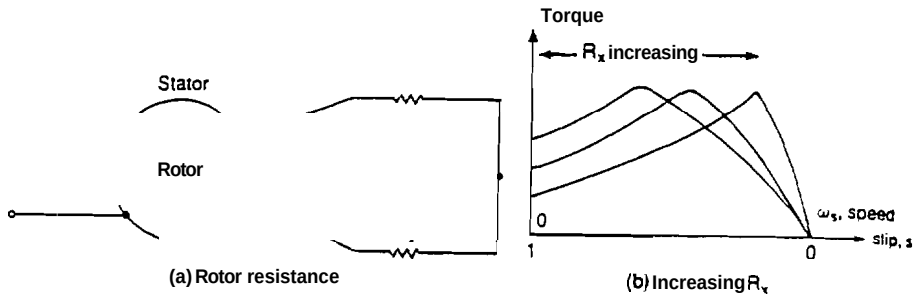

Fig V.3 Speed control by rotor resistance

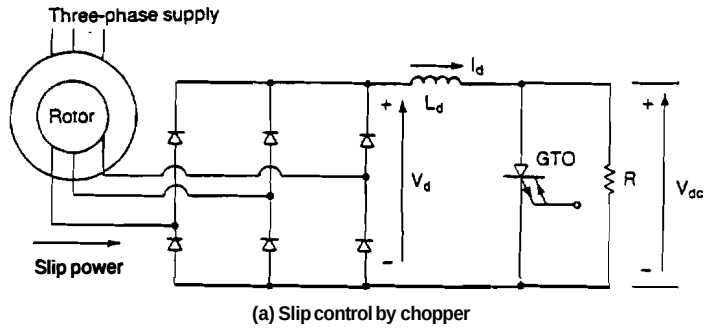

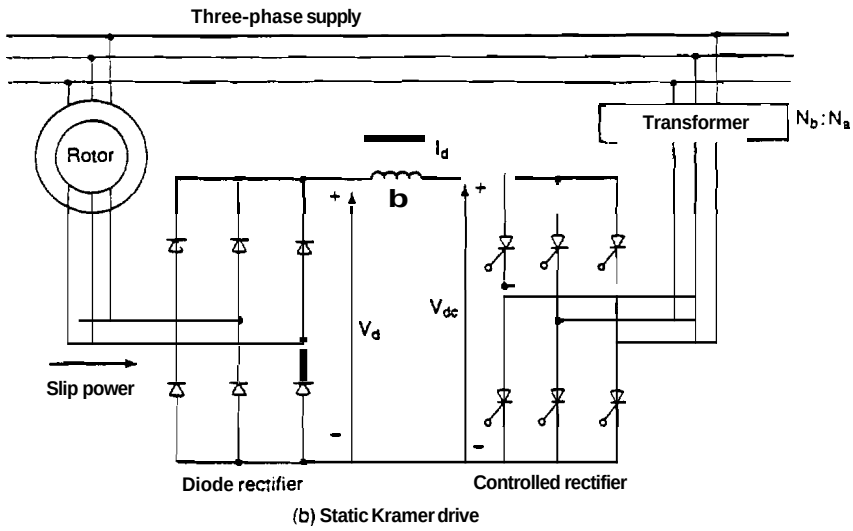

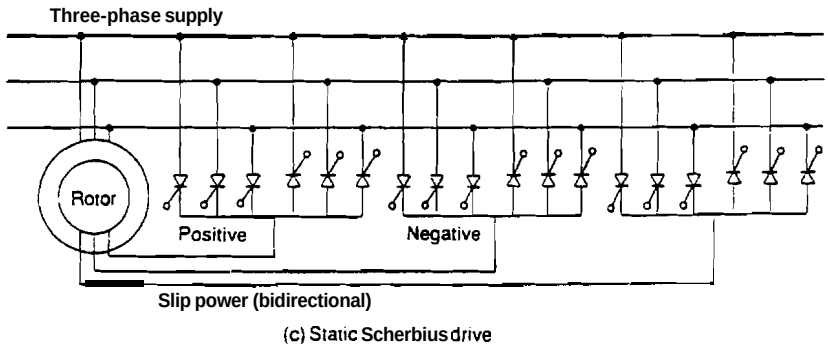

Figure V.4 Slip power control

We can replace the three-phase resistor by a three-phase diode rectifier and a chopper as shown in Fig.V.4.a [2] ,where the GTO operates as a chopper switch. The inductor,L_d, acts as a current source,I_d,, and the chopper varies the effective resistance,

then $R_e=R(1-k)$

where k is the duty cycle of the chopper[2]. The speed can be controllrd by varying the duty cycle.

The slip power in the rotor circuit may be returned to the supply by replacing the chopper and resistance, R, with a three-phase full converter as shown in Fig.V.4.b [2]. The converter is operated in the invertion mode with delay range of $\pi/2 \leq \alpha \leq \pi$, thereby returning energy to the source. The variation of &lay angle permit power flow and speed control.

Again, by replacing the bridge rectifiers by three-phase dual converter (or cycloconverters), as shown Fig.V.4.c [2], the slip power flow in either direction is possible and this arrangement is called a static Scherbius drives.

3). Voltage and Frequency Control

If the ratio of voltage to frequency is kept constant, the flux remained constant. Its characteristics look like[2]

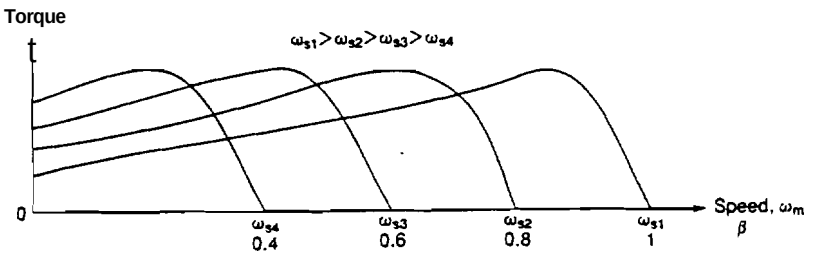

Figure V.5 Torque-speed characteristics with Volts/hertz control

By varying both the voltage and frequency, the torque and speed can be controlled. There are two possible circuit arrangements for obtaining variable voltage and frequency.

In fig. V.6.a [1], the frequency is varied by using a six-step variable voltage input controller. The variable voltage input(VVI) controller used for this duty consists of a phase-controlled.bridge, an auxiliary & cornmutating circuit, and an inverter bridge. Variable voltage is operated by controlling the firing angle of the SCR's in the phas-controlled bridge. This dc

voltage is filtered by a large dc link reactor and capacitor before being inverted into variable frequency ac by the inverter section.

The harmonic voltages associated with the VVI output axe determined by the low output impedance of the voltage source inverter output. Typical voltage and current waveforms are shown in Fig.V.6.b.[3]

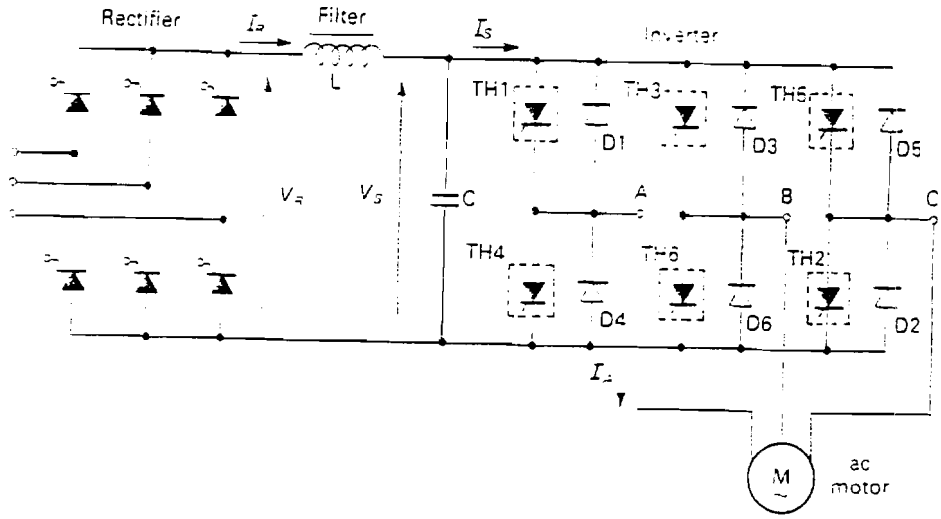

Figure V.6.a Adjustable voltage and frequency controller using controlled thyristo rectifier

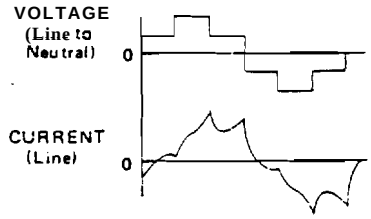

Figure V.6.b voltage and current waveforms using WI controller

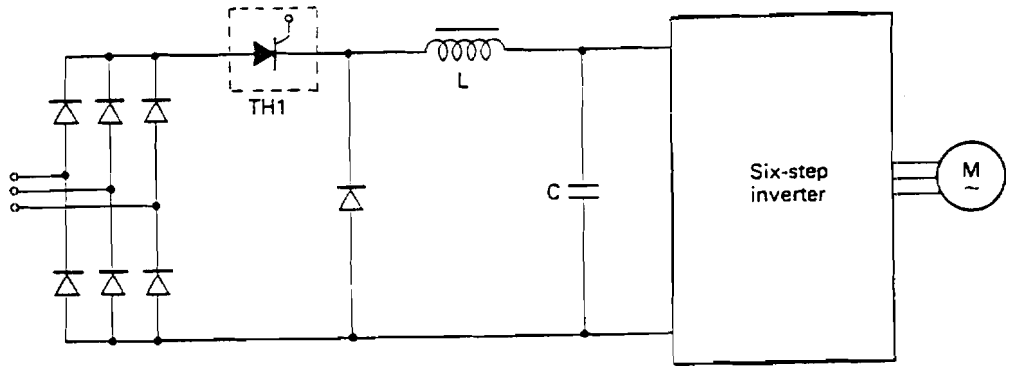

Figure V.6.c Adjustable Voltage and frequency controller using a diode bridge rectifier and dc chopper

Fig.V.6.c shows a six-step inverter drive in which the choppper thyristor TH1 is

alternately gated on and then turned off by the forced commutating circuit. The pulsating output voltage from the chopper is filtered and fed to the six-step inverter, and the average dc voltage is adjusted, by controlling the ratio of on to off-time for the chopper thyristor, and the inverter controls the frequency. Due to the diode rectifier, regeneration is not possible and the inverter wolud generate harmonics into the ac supply.

4). Current Control

In an induction motor drive, there are advantages in controlling stator current rather than stator voltage. Direct control the stator phase currents gives fast, effective control of the amplitude and spatial phase angle of the stator mmf wave, thereby facilitating highquality torque control and rapid dynamic response. Fig.V.7 [2] is the torque-speed characteristics by current control.

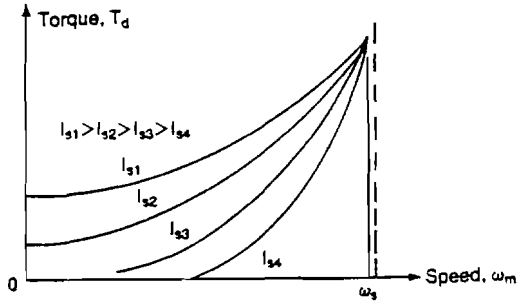

Figure V.7 Torque-speed characteristics with current control

The controlled current can be delivered by a current source inverter. Fig.V.8 [3] shows one configuration of current-fed inverter drive.

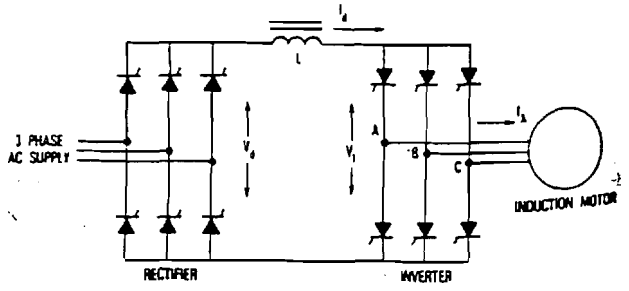

Figure V.8 Variable-current control using controlled current inverter(CSI)

The current sonrce inverter (CSI) controller consists of a phase-controlled bridge and an inverter bridge. Commutation is achieved by means of commutating capacitors and reactors.

Variable voltage is generated by controlling the SCR firing angles. A large dc link reactor then serves as a filter to provide a constant current to the inverter.

The harmonic currents are determined by the inverter output current and have similar content to the harmonics associated with the voltage in the VVI approach. Typical voltage and current waveform are shown in Fig. V.9. [3].

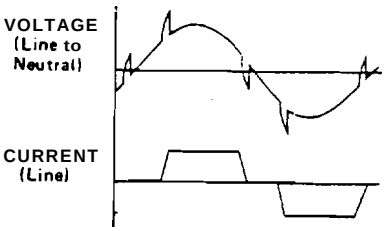

Figure V.9 Voltage and current waveforms using CSI controller

Due to the nonlinear characteristics of static power converter and inverter, the load waveforms are nonsimusoidal. However, these waveforms in the power line are periodic and can therefore be represented by their Fourier series; and, since they have half-wave symmetry, only odd harmonics will be presented, and the waveform can be represented by

$$I(t)=\sum I_k \sin(h\omega t+\theta)$$

$$I_k=I_1/h$$

where, h the order of harmonics, such as 1, 3, 5, 7.....

I1 the amplitude of fundamental current

I_h the amplitude of hrmonic current

These are the thoretical values which no circuit reactance or phase retard exist. However, harmonic current amplitudes are a function of the delay angle(α) and the conmmutating reactance (X_c). The typical values for harmonic analysis are [5]

Harmonic	1	5	7	11	13
Typical value	1	0.175	0.110	0.045	0.029

Then, how do these harmonic currents affect the power systm?

V.3 Harmonics Considerations

With the estimated 400,000 ASDs on-line [7], the harmonic penetration level in the power system is large, and thus the effects on the power system become important. Power system problems such as communication interference, heating, solid-state device malfunction and the high risk of system failure can be the direct result of harmonics. It has been reported power failures due to the system harmonics. On June 24. 1986, the Eurocan Pulp & M i at canada experienced a major failure of its standby incoming 13.8KV utility tie circuit breaker [8]. It resulted in fired and complete destruction of the unit. The investigation showed that the major cause of the circuit failure is the harmonic current.

Table V.l [4] shows some statistics of the system harmonic current distortion due to these non-linear loads, ie., ASDs.

Site: Retail Store In Hays, Kansas				
Distortion:	Vmax: 2.45		Vavg: 1.50	
	Imax: 14.33		Iavg: 9.68	
Sits: Variable speed petroleum pump				
Distortion:	Vmar: 1.88		Vavg: 1.48	
	Imax: 124.06		Iavg: 35.60	
Site: Radio Station, Hays. Kansas				
Distortion:	Vmax: 1.62		Vavg: 1.28	
	Imax: 31.30		Iavg: 16.76	
Site: Liberal arts college				
Distortion:	Vmax: 2.54		Vavg: 1.65	
	Imax: 45.92		Iavg: 19.10	
Slte: Cable manufacturing plant				
Distortion:	Vnax: 2.37		Vavg: 1.43	
	Imax: 12.27		Iavg: 7.50	
Site: Distribution substatlon in Wichita				
Distortion:	Vcax: 4.88		Vavg: 0.94	
	Imax: 23.62		Iavg: 5.17	
Site: Distribution substation in Wichita				
Distortion:	Vmax: 2.19		Vavg: 1.93	
	Imax: 5.68		Iavg: 2.70	
Site: Distribution Substation in Kansas Clty				
Distortion:	Vmax: 3.17		Vavg: 2.19	
	Imax: 13.28		Iavg: 5.71	
Slte: Transmission substation				
Dlstortion:	Vmax: 1.20	Vavg: 0.58		
	Irnax: 7.31	Iavg: 3.05		
Site: Distribution substation				
Distortion:	Vmax: 2.02	Vavg: 1.27		
	imax: 41.75	Iavg: 2.58		

Table V.l Measured current distortion (%THD) in Kansas

We can find that ASDs are the main contributor to the system current distortion.

Today, harmonic considerations for almost any inductrial power system. command almost as much attention as short circuit and overvoltage considerations. An absence of attention to SCR generated harmonics can lead to parallel resonance at generated harmonic frequencies between power factor improvement capacitive reactance and sourc inductive reactance,,resulting in large oscillating current currents and cause equipment insulation failures, capacitor fuse melting, and excessive protective equipment operation.

V3.1 Resonant Circuits

Power systems are made up of inductance, capacitance,and resistance. A combination of inductance and capacitance in either series or parallel sets up a resonance circuit at some frequency. If we only had the fundamental frequency to consider, we could design our power systems to always avoid resonance at this frequency. However, the nonlinearity of static power converters produces equivalent currents of many frequencies. One of these may be near the resonant frequency of circuit components.

The characteristic of parallel resonant circuit is high impedance to the flow of current at the frequency of resonance. A seriers resonant circuit is low impedance to the flow of current at the frequency of resonance.[5]

Let us look at fundamentals, we know that

$$E=IZ$$

where E voltage, I current, Z impedance

For any given I, E is proportional to 2--important in parallel resonance where Z is very high. Likewise

$$I=V/Z$$

For any given voltage, I is inversely proportional to Z--important in series resonance where Z is very low, I is very high. For normal static converter operation, the circuit parameters of inductance, capacitance, and resistance do not combine to be resonant at any characteristic harmonic. Transformer, cable, and dismbution line is small and with normal transformer ,cable, or distribution line inductance. The resonant frequencies are high. The natual frequencies of power circuits are in the kilohertz range [6]. However, when power capacitors are added to the system, the resonant circuits can fall into the range of equivalent frequencies normally encountered with static power converter. The frequency of resonant is

$$f_r = \frac{1}{2\pi}\sqrt{\frac{1}{LC}}$$

where

f_r resonant frequency;

L circuit inductance, H;

C circuit capacitance, F;

V3.2 Determination of harmonic problems

Harmonics produced in the power systems must either be absorbed by the supply system or shorted out by a filter at the load bus. If the amount of harmonic current required by the load is insignificant, the harmonics produced can be ignored. A reasonable calculation to determine the short circuit ratio (SCR) of the system with respect to the static power converter load:

$$\text{Short Circuit Ratio (SCR)} = \frac{\text{system available short circuit (in MVA)}}{\text{total converter rating (in MW)}}$$

If the short circuit ratio is more than 20, the probability of harmonic problems is low [5].

To determine whether the possibility of the harmonic problem such as equipment insulation failures and excessive fuse-blowing, the resonant frequency can also be determined:

$$f_r = f_1\sqrt{\frac{MVA_{sc}}{CMVAR}}$$

where

f_r resonant frequency;

f_1 fundamental frequency, Hz;

MVA_{sc} short circuit capacity of system in MVA;

CMVAR capacitor value in MVAR.

If the harmonic determined by this formular is close to the fifth, seventh, eleventh, or thirteenth harmonics, there is a high probability of producing excessive harmonic voltage and high oscillating harmonic currents. [9].

V.33 Solution

If the determinations indicate the possibility of harmonic problems,, the solution is to provide a low impedance path at the load bus to absorb the harmonic currents injected into the

system. This can be done by providing a circuit consisting of a capacitor and reactor tuned to the frequency of the harmonics. For systems with variable short circuit capacity and switched capacitors, more than one possible offending harmonics may exist For such systems, we should use more filters to eliminate each of them.

Let's look at an exmple [5] of a system using harmonic controlling filters. Fig.V.10 is the one-line diagram of a sysytem which have harmonic problems before fifth and seventh harmonic filters are constructed from the existing capacitor banks by adding reactors.

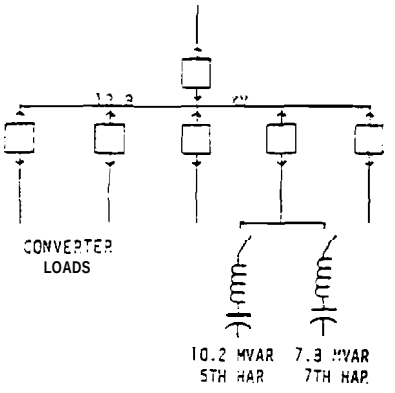

Figure V.10 Simplified one-line diagram of system with have harmon problems before filters are added.

From camparison of Fig. V.11 and Fig.V.12, we can find that tuning the capacitor has reduced the oscillating current and "trapped the harmonic current from the static power converters,. Figs.V.13 and 14 show the improvement in the voltage.

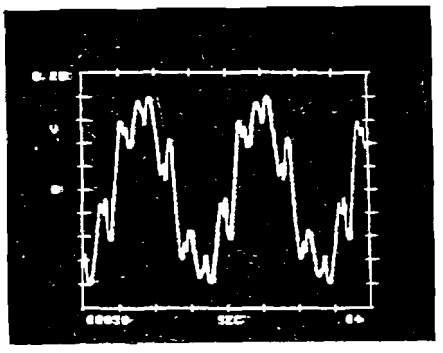

Major harmonics in Dercent of fundamental:

5th	= 24.20	19th	= 3.18
7th	= 24.19	23rd	= 3.02
11th	= 5.87	25th	= 1.93
13th	= 1.82	29th	= 1.63
17th	= 4.64	31st	= 0.85

Figure V.11. Bus B1 capacitor current before filtering

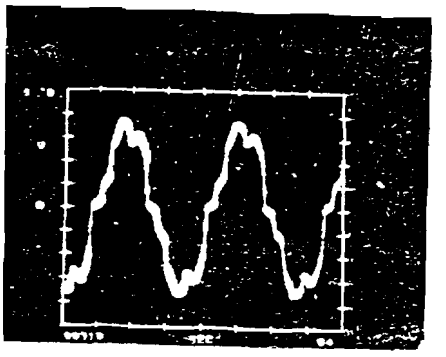

Major harmonics in percent of fundamental:

5th	= 11.96	19th	= 0.66
7th	= 3.00	23rd	= 0.79
11th	= 4.31	25th	= 0.42
13th	= 2.58	29th	= 0.14
17th	= 1.22	31st	= 0.23

Figure V.12 Bus B1 capacotor current after filtering

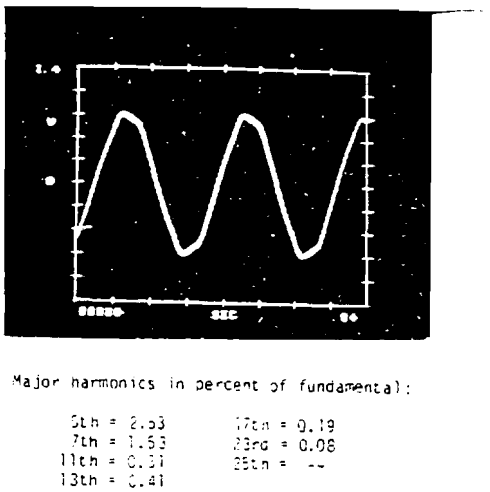

Figure V.13 Bus **B1 voltage before filtering**

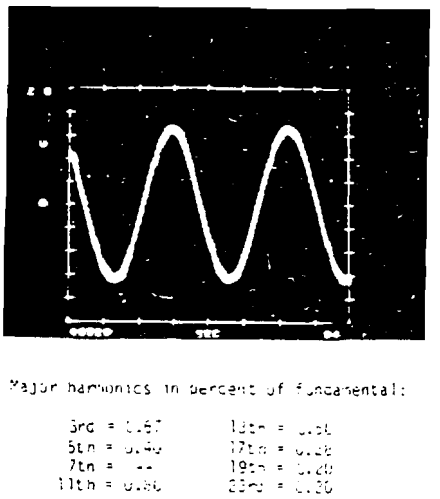

Figure V.14 Bus **B1 voltage** after **filtering**

V.4 Summary

The technology of adjustable-speed drive grows rapidly. It has a significant impact on the performance and cost-effectiveness of the modem ac drive system. As a result, there is now a rapid expansion in inductrial application of the ac drive, and this growth is being accelerated by a greater recognition of the enhanced performance capability. However, the adjustable-speed drive is also a generator of harmonic currents of the system. More attention must be paid on the effect of ASD to the power system and find ways to reduce the effect. One way is to &sign and add the harmonic filters to the circuit to prevent any excessively high harmonic voltages or voltage distortion, and to prevent any fuse-blowing from high oscillating harmonic currents.

V.5 References

[1] Murphy, J.M.D.," Power Electronic *Control* of AC *Motors"*, Oxford; New York: Pergamon,1988

[2] Rashid,M.H.,"*Power Electronics:Circuits,Devices,and* Applications", Englewood Cliffs, N.J.:Prentice Hall,1088

[3] Connors, Dennis P.," *Considerations* in Applying Induction Motors with *SolidState* Adjustable Frequency *Controlers*", IEEE Trans. Ind.Appl. IA20, 1, Jan./Feb. 1984, pp113-121

[4] Jewell, Word T.,Egbert, Robert I.,"*A study* of *Harmonics* in *Kansas* Utility .Systems", Third International Conference on Harmonics in Power Systems, Purdue University, Sept, 1988, pp66-72

[5] Smith, R.L., and Straford, R.P.," Power System *Harmonics Effects from AdjustableSpeed* Drives", IEEE Trans.Ind.Appl. IA20,4,July/Aug.1984 ,pp973-977

[6] Stratford,R.P.,"*Rectifier Harmonics* in Power *Systems*",IEEE Trans.Ind.Appl., IA16,2,Mar./Apr.1980 ,pp71-80

[7] A.Domijian, Jr:," A Summary and Evaluation of Recent Developments on *Harmonic Miligation* Techniques Useful to Adjustable Speed Drives", IEEE trans. Energy Conversion Jan./Feb. 1992, pp64-71

[8] Oliver, J.A., Samotyj, M.J.,"*Experience with Large* Adjustable Spee Drives in Power *Plants*",Third International Conference on Power Electronics and Variable Speed Drives: Jul.1988 London:Institution of Electrical Engineers,IEE Conference Publication,No.291,1988, pp13-15

[9] Jr, Robert L.Smith, "*Application* Considerations in Handling *Efects* of *SCR* Generated Harmonics in *Cement* Plants", IEEE Trans.Ind.Appl. IA 17,No.1,Jan./Feb.,1981, pp63-70

CHAPTER VI

MEASUREMENT OF POWER QUALITY

Brian H. Kwon

VI.1 Introduction

Power quality is the maintenance of proper voltage and frequency of an electric power source. Power quality is of concern to industry, as a result, this is a topic which is of considerable interest in industry at this time.

According to Electric Power Research Institute (EPRI), over 1 billion dollar is spent by the electric utility industry each year to maintain, enhance, and analyze power quality in the United States.[5]

In an ideal electrical power system, energy is supplied at a single and constant frequency, and at a specified voltage levels of constant magnitude. However, the uses of nonlinear loads to the system such as static power converters, arc discharge devices, saturated devices change the sinusoidal nature of the ac power, thereby resulting in the flow of harmonic currents in the ac power system which can interfere the communication circuits and other types of equipment.[4]

Power system distortion is not a new issue for many engineers and has been a concern of power engineers from the early days. The goal for this paper is to define some electric power quality indices and to look at some instruments that measures the electric power quality.

VI.2 Power Quality Indices

There has been many issues related to harmonics in power systems which threaten the quality of the electric power supplied to the consumer. As a good example, IEEE standard 519-1992 was issued to constrain the limits on harmonic distortion and to obtain a high power quality. This standard is only a guide, however, many industries are using this for the recommended practice. The recommended practice is to be used in the design of power system with nonlinear loads. The limits set are for steady-state operation and are recommended for "worst case".

There are two criterions that are used to evaluate harmonic distortion condition. The first is a limitation in the harmonic current that a user can inject into the network. The second is the quality of the voltage that the industry must provide to the user. *[5]*

The IEEE Standard 519 puts two limits on the harmonic current distortion. First, limits on the individual harmonic currents generated by the user. Second, limits on the current Total Harmonic Distortion (THD) at the load bus. The THD is usually expressed as a percent of the fundamental. Current Total Harmonic distortion is given by [5]

$$I_{THD} = \frac{\sqrt{\sum_{h=2}^{\infty} I_h^2}}{I_1} \qquad \text{(VI.1)}$$

where

I_h : the amplitude of the harmonic current of order h

I_1 : the amplitude of the fundamental current.

Table (VI.1) list the current distortion limits for general distribution system.[5] By distribution system, it means from 120v through 69000v. For the subtransmission, or transmission system, these values are slightly different. Commonly, cited figure of 5% is dividing line between high and low distortion. However, 5% in harmonic distortion in subtransmission and transmission circuits is usually too high to be tolerated. In this table, the rate of I_{sc}/I_1 is the ratio of the short circuit current available at the point of common coupling to the nominal fundamental current. [1]

I_{SC}/I_1	Harmonic Current Distortion (%)				
	Harmonic Order				Total Harmonic Distortion
	<11	11-22	23-35	>35	
<20	4	1.5	1.0	0.5	5.0
20-49.9	7	2.5	1.5	0.8	8.0
50-99.9	10	4.0	2.0	1.2	12.0
100-1000	12	5.0	2.5	1.5	15.0
>1000	15	8.0	4.0	1.8	20.0

Table (VI.1): Limits of Current Distortion

Harmonic Voltage Distortion (%)			
	2.3-68.9 KV	69-138 KV	>138 HN
Maximum For Individual Harmonic	3.0	1.5	1.0
Distortion (THD)	5.0	2.3	1.5

Table (V1.2): Limits of Voltage Distortion

The second limitation, as mentioned above, the quality of voltage that the utility must provide to the user. The IEEE Standard 519 specifies limits on the bus voltage of the individual harmonics as well as on the bus voltage Total Harmonic Distortion. It is given as [5],

$$V_{THD} = \frac{\sqrt{\sum_{h=2}^{\infty} V_h^2}}{V_1} \qquad \text{(VI.2)}$$

where

V_1 : the amplitude of fundamental voltage

V_h : the amplitude of harmonic voltage of order h.

Table (VI.2) lists the voltage distortion limits for distribution, subtransmission and transmission system.[5] While there is no definite rule as to where the truncation point of the infinite series in the definition for THD may be made, there are some guidelines: the ANSI standards take a conservative stance and recommended truncation of the series at 5kHz. However, most practical, commercially available instruments are limited to about 1.6kHz due to the voltage and current transformers used and due to the word.length of the digital hardware. One disadvantage about THD is that it does not show the amplitude of voltage and current. [I]

There are many problems caused by harmonics in power system. Perhaps the most serious problem is the coupling between power and communication circuits.[4] One representation of measuring these problem is the Telephone Influence Factor (TIF). TIF is a dimensionless value that often used to describe the interference: of a power transmission line on the telephone line. In many places, telephone circuits are now pulse code modulated, and the TIF will not indicate the interference level between power circuit and a PCM circuit. However, many local telephone services are simply analog in nature, and the TIF is useful for assessing interference in such cases. The high weighting

factors are given to the harmonic frequencies which are sensitive to the hurnan ear. TIF for voltage v(t) is expressed as following [5]:

$$TIF = \frac{\sqrt{\sum_{h=1}^{\infty}(w_h V_h)^2}}{V_{RMS}} \qquad (VI.3)$$

where

V_{RMS} : the root mean square voltage of the bus

w_h : the TIF weighting coefficient at harmonic h

The infinite sum in the TIF definition is recommended to truncate at 5.0 kHz according to the ANSI standard 368 but a much lower truncation is often used in actual. practice.[1] Table (V1.3) lists the TIF weighting coefficients.[5] From the inspection of the TIF weights., it shows that the audio characteristic is most sensitive in the frequency band 2400 - 2880 Hz. The weights for frequencies which are more usually used in power quality measurement are about two orders lower than those of cited band. However, the magnitude of the harmonic signals in power system below thirteenth harmonic are usually about an order of magnitude lower than those regularly encountered in the band 2400 - 2880 Hz.[1]

Another power quality index that are often used is called C-message weights. They are used to get a reasonable indication of noise interference on the telephone line from each power system harmonics. In 1960, the Bell Telephone System (BTS) revised the C-message weight that had been published in 1919. The C-message weighted index for current i(t) is defined as [1],

$$C = \frac{\sqrt{\sum_{h=1}^{\infty}(c_h I_h)^2}}{I_{RMS}} \qquad (VI.4)$$

where

I_{RMS} : the root mean square current

c_h : the C-message weighting coefficient at harmonic h

h	f(Hz)	C-msg	TIF	h	f(Hz)	C-msg	TIF
1	60	0.0017	0.3	26	1560	0.871	6790
2	120	0.0167	10	27	1620	0.860	6970
3	180	0.0333	30	28	1680	0.840	7060
4	240	0.0875	103	29	1740	0.841	7320
5	300	0.1500	225	30	1800	0.841	7570
6	360	0.222	400	31	1860	0.841	7820
7	420	0.310	650	32	1920	0.841	8070
8	480	0.396	950	33	1980	0.841	8330
9	540	0.489	1320	34	2040	0.841	8580
10	600	0.597	1790	35	2100	0.841	8830
11	660	0.685	2260	36	2160	0.841	9080
12	720	0.767	2760	37	2220	0.841	9330
13	780	0.862	3360	38	2280	0.841	9590
14	840	0.912	3830	39	2340	0.841	9840
15	900	0.967	4350	40	2400	0.841	10090
16	960	0.977	4690	41	2460	0.841	10340
17	1020	1.000	5100	42	2520	0.832	10480
18	1080	1.000	5400	43	2580	0.822	10600
19	1140	0.988	5630	44	2640	0.804	10610
20	1200	0.977	5860	45	2700	0.776	10480
21	1260	0.960	6050	46	2760	0.750	10350
22	1320	0.944	6230	47	2820	0.724	10210
23	1380	0.923	6370	48	2880	0.692	9960
24	1440	0.924	6650	49	2940	0.668	9820
25	1500	0.891	6680	50	3000	0.645	9670

h = harmonic of 60 Hz

f = frequency

C-msg = C-message weights

TIF = Telephone Influence Factors

Table (VI.3): TIF and C-message Weighting Coefficients

Table (VI.3) lists also the C-message weighting coefficient.[5] The C-message weight is very much similar to TIF except the weights c_i are used instead of w_i. These weights are related as follows [1],

$$5if_o c_i = w_i \tag{VI.5}$$

The TIF weights account for the fact that mutual coupling between circuits increases linearly with frequency, while the C-message weights are free of this fact assuming that the mutual inductances between adjacent circuits is essentially frequency independent.

In Europe, the harmonic Distortion Index, DIN, is used to measure of the power system harmonic content. DIN is defined as [1],

$$DIN = \frac{\sqrt{\sum_{h=2}^{\infty} V_h^2}}{V_{RMS}} \tag{VI.6}$$

where

V_{RMS} = the root mean square of the bus voltage.

$$= V_1^2 + \sum_{h=2} V_h^2$$

Using this equation, the relationship between DIN and THD can be found as follows,

$$DIN^2 = \frac{\sum_{h=2}^{\infty} V_h^2}{\sum_{h=1}^{\infty} V_h^2} \tag{VI.7}$$

$$= \frac{\sum_{h=2}^{\infty} V_h^2}{V_1^2 + \sum_{h=2}^{\infty} V_h^2} \tag{VI.8}$$

Since $\sum_{h=2} V_h^2 = V_1^2 * (THD)^2$, (VI.9)

$$DIN^2 = \frac{V_1^2 * (THD)^2}{V_1^2 + V_1^2 * (THD)^2} = \frac{THD^2}{1 + THD^2} \tag{VI.10}$$

Take the square root on both sides,

$$\text{THD} \tag{VI.11}$$

or

$$\text{THD} = \frac{\text{DIN}}{\sqrt{1 - (\text{DIN})^2}} \tag{VI.12}$$

For low levels of harmonic distortion, one can apply Taylor series expansion for expressions of the form $\frac{1}{(1+\varepsilon)}$ and $\sqrt{1+\varepsilon}$, which are $1-\varepsilon$ and $1+\frac{E}{2}$ respectively; then, DIN $\approx$ THD * $(1 - \frac{1}{2}(\text{THD})^2)$. For small THD less than 5 %,

$$1 >> \frac{1}{2}(THD)^2 \tag{VI.13}$$

Then, THD and DIN become almost equal. From looking at above equations, we could say that the THD determines the DIN or the other way around. The only advantage of one over the other depends on the individual. The DIN becomes unity for a highly distorted wave but the THD becomes infinite. Some engineers put more importance on one of these indicative levels for this circumstances. Figure (VI.l) shows the relationship between DIN and THD for the different level of distortion.[1]

Other often used power quality indices are I·T and KV-T product. I·T product is the inductive influence in the power system and is defined as follows,[1]

$$I \bullet T = \sqrt{\sum_{h=1}^{\infty}(w_h I_h)^2} \tag{VI.14}$$

$$= I * (TIF_I) \tag{VI.15}$$

where

w_h : the TIF weights

I_h : the nns current at frequency f

KV-T product is the inductive influence in terms of the product of its root-mean-square magnitude, in kilovolts, times its telephone influence factor (TIF).

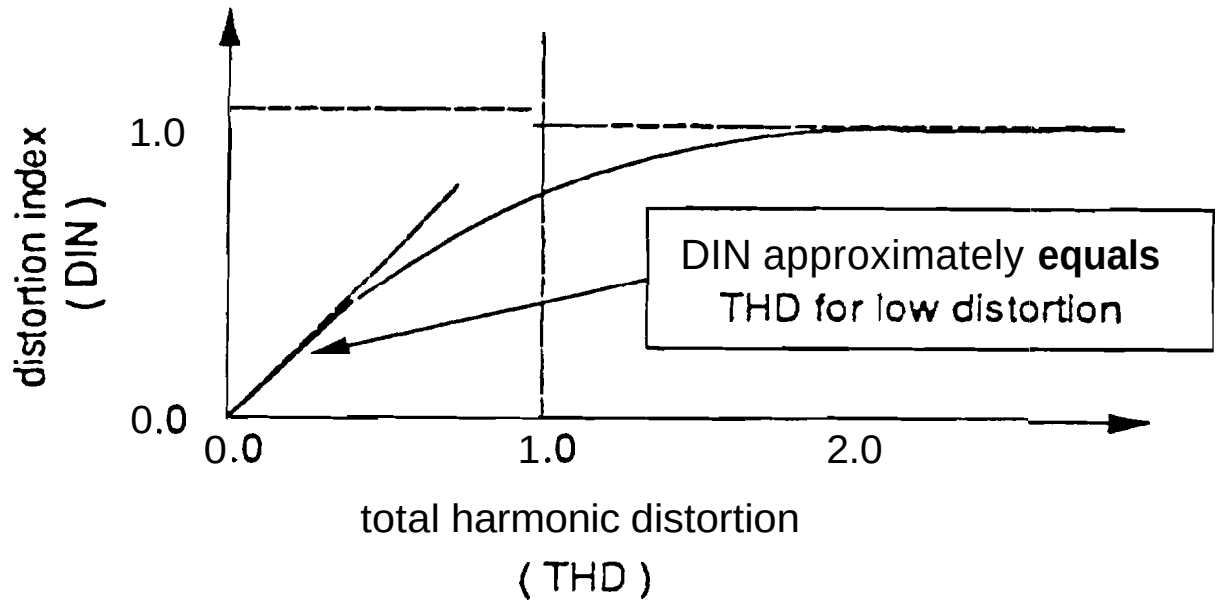

Figure (VI.1) : Total Harmonic Distortion vs. Distortion Index

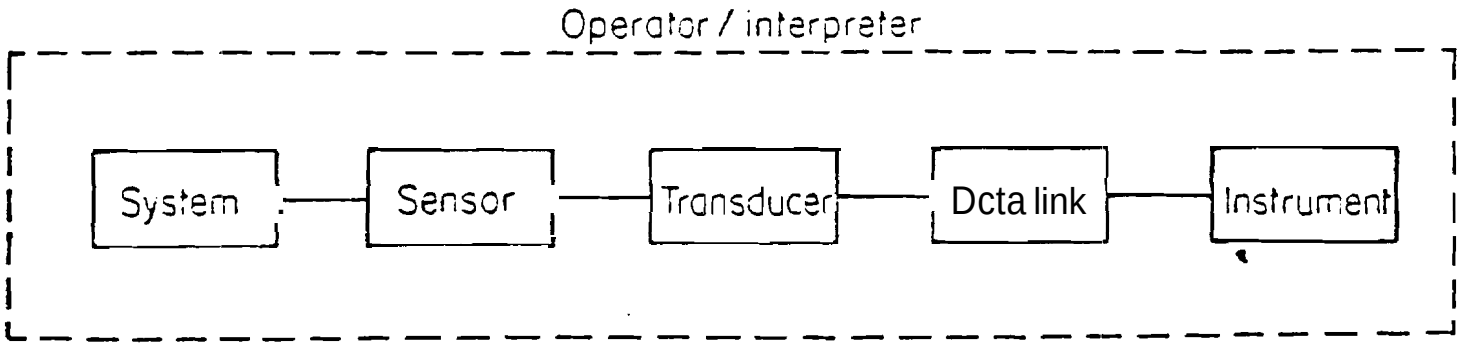

Figure (V1.2): Measurement System

VI.3 Power Quality Measuring Instrument

To maintain an efficient and effective electricity supply, it is necessary to define the levels of distortion that can be permitted on the power system. This need has resulted to the development of a series of measuring instruments and techniques of steadily increasing sophistication which leads to the microprocessor-based measuring equipment.

Any measuring system is formed by the appropriate connection of a number of component parts as illustrated by Figure (VI.2).[2] The actual combination will vary a little bit for different systems. The role of this operator/interpreter is establish the need for information, then the measurement required to provide this information is identified by determining whether full or partial harmonic spectra, simultaneous measurements of current and voltage, harmonic power and power flow, single or multiphase measurement or other related factors. After identifying the measurement parameters, the measuring system can be identified.[2]

There are some basic instruments used for the analysis of non-sinusoidal voltage and currents. These are the following [3]:

Oscilloscope - The display of the waveform on the oscilloscope gives immediate qualitative information on the degree and type of distortion. Sometimes cases of resonances are identifiable through the visisble distortion that is present in the current and voltage waveforms.

Spectrum Analyzers - These scan a range of frequencies to provide a measurement of signal amplitude at all frequencies within that range. In other word, these display the power distribution of a signal as a function of frequency. All the components, harmonics, and interharmonics of the analyzed signal are displayed. The display format may be a CRT or a chart recorder.

Harmonic Anaylizers - These measure signal amplitudes at harmonic frequencies only. In order to achieve this the measurement is referenced to the fundamental frequency

and allowance made for any variation in that frequency. The harmonic analyzer provides an output spetrum which is a specific subset of the spectrum of siganl amplitudes that would be produced by a spectrum anlayzer covering only the frequency range containing the harmonics. The output can be recorded, or it can be monitored with analog or digital meters.

Distortion Analyzers - These indicate THD directly.

Digital Harmonics Measuring Equipment - Digital Analysis can be done with two basic ways:

(1) By means of digital filter. - this is similar to analog filtering. Dual-channel digital signal analyzers include digital filtering. In the setup for a particular measurement, the frequency range to be measured sets up the digital filters for that range. In addition, the bandwidth is varied to optimize the capture of smaller harmonics in the presence of a very large fundamental.

(2) The Fast Fourier Transform technique - These are real-time, very fast methods of performing a spectrum analysis that permit the evaluation of a big number of functions. Multichannel analog-digital conversion and micro or mini computers are used for real-time data acquisition.

VI.4 Example Calculation of Power Quality Indices

To illustrate an example in calculating the power quality indices we have the following problem: A purely resistive load is located at a 69kV substation bus. At the substation, the measured bus voltage was 69.1 kV and the fundamental load power is 16 MVA at unity power factor. Also, the third harrnoinic voltage measured was 1.0 kV line-

to-line, and the fifth harmonic voltage measured was 500 V. Find the THD, TIF, C-message weight, and DIN for both the voltage and load current. In addition, find the K·VT and I·T products. Assume that system is 60 Hz.

First, find the fundamental current, whch is,

$$|I_1| = \frac{P/3}{V/\sqrt{3}} = \frac{16MVA/3}{69.1kV/\sqrt{3}} = 133.68 \text{ Amperes per phase}$$

The load resistance is

$$R = \frac{69.1*10^3/\sqrt{3}}{133.68} = 298.42\ \Omega \text{ per phase}$$

Using Ohm's law, the amplitude of third and fifth harmonic currents are founcl,

$$I_3 = \frac{1000/\sqrt{3}}{298.42} = 1.935 \text{ Amperes/ phase} \qquad I, = \frac{500/\sqrt{3}}{298.42} = 0.967 \text{ Amperes / phase}$$

The THD's for the voltage and current are then found,

$$V_{THD} = \frac{\sqrt{0.5^2 + 1.0^2}}{69.1} * 100 = 1.62\ \% \qquad I_{THD} = \frac{\sqrt{0.967^2 + 1.935^2}}{133.68} * 100 = 1.62\ \%$$

The TIF weights for 60, 180, and 300 Hz respectively are 0.5, 30, and 225. The TIF for the voltage and current are same and I have calculated for the voltages,

$$TIF, = \frac{\sqrt{((0.5)*(69.1))^2 + ((30)*(1.00))' + ((225)*(0.5))^2}}{\sqrt{69.1^2 + 1.0^2 + 0.5^2}} = 1.7574$$

The C-message weight for 60, 180, 300 Hz respectively are 0.0017, 0.0333, and 0.15. The C-message weight index for the voltage and current are same and I have calculated for the current,

$$C_I = \frac{\sqrt{((0.0017)*(133.68))^2 + ((0.0333)*(1.935))^2 + ((0.15)*(0.967))^2}}{\sqrt{133.68^2 + 1.935^2 + 0.967^2}} = 0.0021$$

The DIN are found, however, the D M for the voltage and current are same and can be checked by the Equation (VI.11). Using the THD calculated above, I have calculated the DIN,

$$DIN = \frac{0.0162}{\sqrt{1 + 0.0162^2}} * 100 = 1.619\ \%$$

The individual K·VT and I·T products are found using the TIF weights.

K·VT product	**I·T product**
60 Hz (0.5)*(69.1) = 34.55	60 Hz (133.68)*(0.5)*$\sqrt{3}$ = 115.77
180 Hz (30)*(1.00) = 30.00	180 Hz (1.935)*(30)*$\sqrt{3}$ = 100.55
300 Hz (225)*(0.5) = 112.50	300 Hz (0.967)*(225)*$\sqrt{3}$ = 376.85

$$K \bullet VT_{\text{„}} = \sqrt{34.55^2 + 30' + 112.5^2} = 121.44$$

$$I \blacksquare T_{total} = \sqrt{115.77^2 + 100.55^2 + 376.85^2} = 406.85$$

VI.5 Conclusion

I have defined some power quality indices and listed some instruments that measure the power quality. The power quality indices listed were THD, TIF, C-message Weight, DIN, I·T product, KV·T product. Perhaps the most often used index is THD and some of the properties of the THD are as follows:

1) The THD is zero for a perfectly sinusoidal waveform.

2) As the distortion increases, the THD becomes indefinitely large

3) It does not show any information about the amplitude of voltage and current.

For accurate harmonic measurements, the instrument must perform the measurement of a constant harmonic component with an error compatible with the permissible limts. It is also necessary to select the instrument based on the indication of its ability to separate harmonic: components of different frequencies. In addition, since the bandwidth of the instrument will strongly affect the reading when harmonics are fluctuating, it is recommended that instruments with a constant bandwidth for the entire range of frequencies to be used.[3]

The measurement of harmonics in power system has been considerable significance because the need of monitoring the power system harmonic contents and evaluating the harmonic distortion factors to check their compliance with the IEEE Standard. As far as I am concern, this practice should be familiar to all power engineers. From the previously defined the power quality indices, perhaps it would nice to define new power quality indices to further develop the power quality in the near future.

VI.6 References

[1] G.T. Heydt, Electric Power Quality, Stars in a Circle Publications, 1991.

[2] Arrillaga, J., Bradley, D.A., and Bodger, P.S., Power System Harmonics. New York: John Wiley & Sons, Wiley Interscience, 1985.

[3] IEEE Std 519-1992, IEEE Recommended Practices and Requirements for Harmonic Control in Electrical Power Systems (ANSI).

[4] "Coordination of Power and Communication Systems", by R.D. Evans, Westinghouse Engineer. TRANSMISSION AND DISTRIBUTION.

[5] Beides, Husan Mohamed, "Dynamic State Estimation of Power System Harmonics", Thesis 1991.

Chapter VII
Lightning Induced Voltages on Overhead Distribution Lines

Dan Hu

VII.1 Introduction

Lightning is an electrical discharge in the air between clouds, between separate charge centers in the same cloud, or between cloud and earth. Only the last case may cause damage on power systems. Lightning is the leading cause of damaging overvoltages on distribution systems, because the insulation level of distribution is low[5]. It has been considered that lightning damages on distribution lines are caused by indirect strokes as well as direct strokes. However, experimental studies [2] indicate that indirect stroke events, although less energetic than direct strokes, may be a significant problem due to their high frequency of occurrence.

Lightning is still more or less unpredictable. Different strokes may vary greatly in the amplitudes and wave shapes of surge currents which they produce as well as in their durations and multiple character, and produce different inducted voltages on overhead distribution lines. The amplitudes of induced voltages may also differ in different lightning ground flash positions. However, based on statistical data, it is possible to study the general characteristics of lightning surges and the inducted voltages which they produce on overhead distribution lines.

The objective of this paper is to study the generation, characteristic and damages of lightning inducted voltages on overhead distribution lines, and some methods to improve the lightning performance are also discussed.

VII.2 Lightning surges

The knowledge of lightning characteristics is essential for understanding the cause of lightning impulses on overhead lines. The following discussions are the important characteristics of lightning and the effects of lightning surges on overhead distribution lines.

VII.2.1 Mechanics of a lightning flash

The general pattern of a thundercloud is shown in Figure VII.1[3]. Positive charges are located in the top region of the thundercloud, and the negative charges are in the lower region. Those negative charges induce positive charges on the earth's surface. As the charges increase, the potential between the cloud and the earth increases, the electric field also increases. When field strength exceeds the critical breakdown level, the lightning discharge begins.

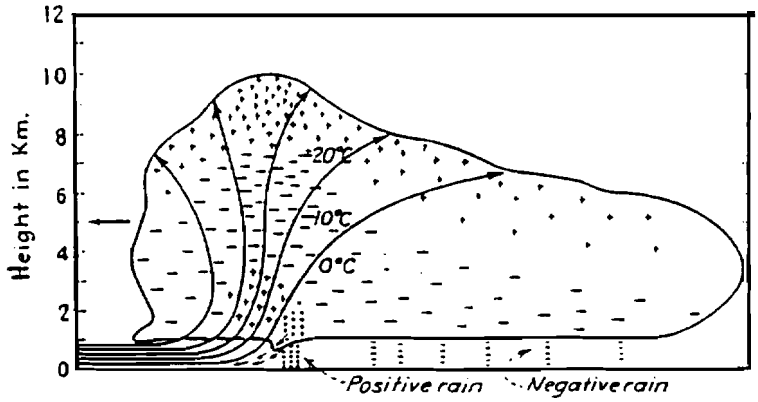

FIGURE VII.1 Electrically charged cloud

The first stage of a lightning stroke is shown in Figure VII.2.(a)[3]. The leader stroke of negative charges advances downward, from the cloud to the earth. The leader stroke's average velocity of propagation is about 1E+7 to 2E+8 cm/s[3]. The voltage between the lightning cloud and the ground is between 10 and 100MV, and the field strength may reach 50-300kV/m near the earth's surface[9]. During the progression of the leader stroke, a streamer discharge develops from the earth's surface and grows upward to meet the downcoming leader, FigureVII.2.(b). This return stroke which consists of positive charges flows upward to neutralize the existing negative charges, Figure VII.2.(c)(d). This contact is like the closing of a switch between the two opposite charges. At this moment, the high current associated with lightning occurs. The initial return stroke travels along the return channel much faster than the speed of the leader. It usually builds up from zero to its crest in a few microseconds and then decays quickly, but more slowly than it rises. Table VII.1 gives measured and estimated results of lightning parameters.

Actually, this charged and discharged process may be repeated over and over, so that what

appears to the eye as a single flash is really made up of a number of strokes, Figure VII.2.(e)(f). Sometimes negative lightning surges may occur due to positively charged clouds. However, the frequency of occurrence of this kind of surges is less than 10% [7]. Therefore, most research only focuses on positive surges.

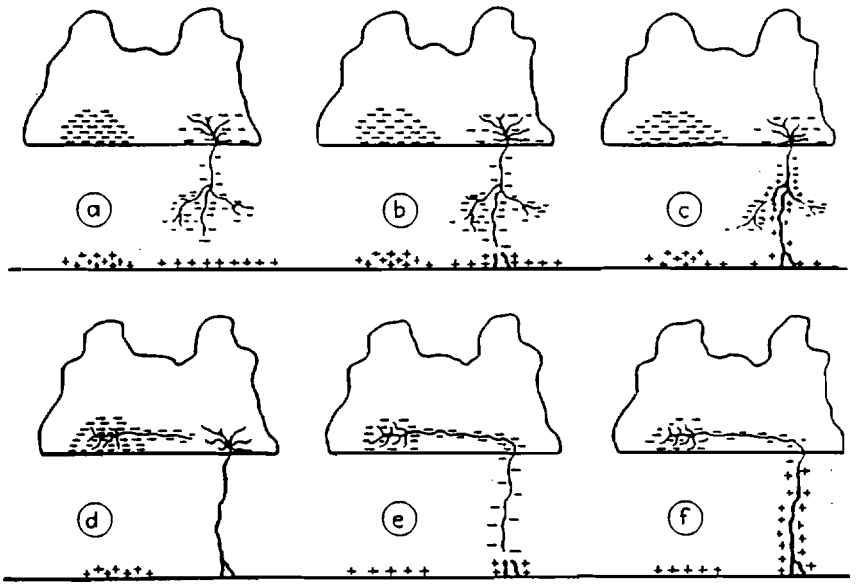

Figure VII.2 Formation of lightning surge.

Parameter	In free space
Voltage (MV)	10–20–100
Field strength (kV/m)	50–200–300
Time duration (μs): Front rise	5–10–20
Back decay	
Current strength (kA)	10–100–500
Temporal behavior	Mostly overdamped
Spatial extent (km)	0.2–2–4

Table VII.1. Measured and estimated lightning parameters

VII.2.2 The amplitudes and wave shape of lightning surge currents

In order to establish the amplitudes of induced overvoltages on distribution lines as a result of lightning, it is essential to understand the amplitude and waveshape of lightning surge currents. Although there is not one standard lightning stroke, it is possible to construct a general wave

shape for stroke currents based on a large number of observations. According to the model of lightning surge currents discussed in [9], the amplitude of a stroke current can be obtained by using the following formula,

$$I = \frac{D}{4\sqrt{2}v\sqrt{\ln\frac{D}{d} - \frac{1}{2}}} \cdot \frac{E}{a}$$

Where c -- the velocity of light

v -- the potential difference between the two condenser plates, namely the cloud and the ground or lines

D – the diameter of the charged cloud (in kilometer)

d -- the diameter of the stroke

E/a -- the average breakdown-voltage field strength in the air

The general wave form for lightning surges is shown in Figure VII.3 [8]. The wave front of the discharged current exists about 1-10 microseconds and the entire duration may approach 100-1000 microseconds. The amplitude of surge currents may reach 100 -500kA. Therefore, a lightning stroke can be treated as a current pulse with high amplitude.

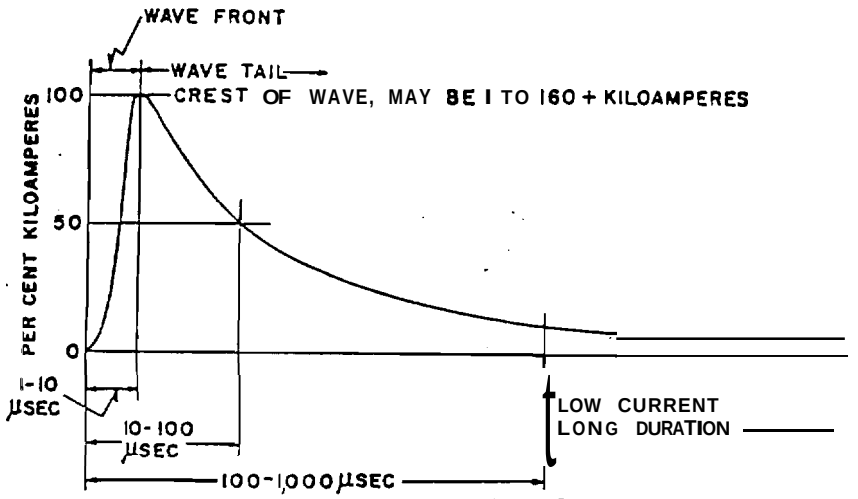

FIGURE VII.3 **Generalized wave shape of lightning-stroke current**

VII.3 Induced voltage on overhead distribution lines

From the discussion above, it can be seen that lightning need not come in direct contact with power lines to cause problems, since induced charges can be introduced into the system from nearby lightning strokes to the ground. It has been investigated that for lines of 6.6kV or below indirect stroke events may be a significant problem because of their high frequency of occurence[2].

As the stroke leader approaches the earth, the electrostatic and electromagnetic fields associated with the main stroke discharge may induce potential in nearby lines. Voltage induced on the line will propagate along the line in the form of a traveling wave until dissipated by attenuation, leakage, insulation failure, or surge-arrester operation.

Induced voltages caused by indirect lightning surges on overhead distribution lines are impulses. There are many factors that may affect their amplitudes. Besides the lightning currents discussed above, the positions of the lightning flashes, the configuration of overhead distribution lines, and the: manner of progress of lightning flashes are also very important.

VII.3.1 Induced voltage Model

The complexity of the lightning flash makes accurate modeling very difficult. In general, the amplitude of induced voltage is considered a function of the following parameters: the peak and the time to crest of the return-stroke current, return-stroke velocity, line height, and perpendicular distance of the stroke point from the lines.

A number of theoretical analyses and experimental studies on the interaction between lightning and distribution lines have been carried out [2] [4][6][7], but some differences in predicted induced voltage still exist. Among those models, the Eriksson's model is one of the most notable. His model is based on the following assumptions:

(1) Only the electrostatic and electromagnetic components associated with the lightning return stroke are significant. Bound charges and the effects of the creation of the stepped leader are

ignored.

(b) The conductor is loss-free and of constant height above a perfectly conducting earth.

(c) The height of the overhead line is small compared with the distance of a flash from the line.

(d) The Length of the overhead line is infinite, so the bound effect can be ignored

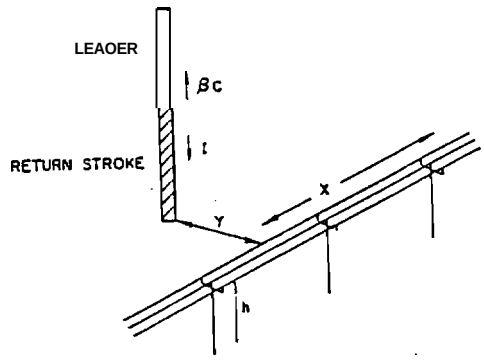

FIGURE W.4 Return-stroke model geometry.

Therefore, the induced voltage V, at time t and at point x on the line (Figure **VII.4)** is given by the forced wave equation:

$$V = U(x) + U(-x)$$

where $$U = Z_0 I h \beta \left\{ \frac{ct - x}{y^2 + \beta^2 (ct - x)^2} \right\} \times \left\{ 1 + \frac{[\beta^2 ((ct - x) + x)}{\sqrt{\beta^2 c^2 t^2 + (1 - \beta^2)(x^2 + y^2)}} \right\}$$

where c -- velocity of light in free apace

βc -- velocity of return stroke

I -- return stroke current

and $$Z_0 = 1/4\pi\sqrt{\mu_0/\varepsilon_0} \equiv 30\Omega$$

The peak voltage Vp is given by

$$V_p = Z_0 I h \left\{ \frac{1}{2y} \times \left[1 + \frac{(x + \beta y)}{\sqrt{x^2 + 2y^2 + 2\beta xy - \beta^2 y^2}} \right] \right\}$$

$$\times \frac{(2\beta x + y)}{[y^2 + (2\beta x + y)^2]} \times \left[1 + \frac{(2\beta^2 x + \beta y - \beta x)}{\sqrt{(x^2 + 2y^2 + 2\beta xy - \beta^2 y^2)}} \right]$$

The relations between B and I are assumed as following:

$$\text{where} \qquad \beta = 0.0041 I^{0.64} + 0.068$$

$$\beta = 0.004 I^{0.086} + 0.18$$

This is a simple model for the calculation of induced voltages in a distribution line. However, a distribution system is much more complex. It contains not only single-phase lines but also two-phase and three-phase lines. Some of these lines are shielded by overhead earth wires. In such cases, this model should be modified.

Some experiments show that the median amplitude of induced voltages on distribution lines is a range of 25-30kV[8], and few overvoltages exceed 300kV[4].

VII.3.2 The wave shape of induced voltages

The general wave form of induced voltages is similar to that of Lightning surge currents.It is shown in Figure VII.5 [8]. The portion of the wave from its beginning to its crest is called the wave front. The decaying part after the crest is passed is called the wave tail. The scale of the vertical axis is per unit of induced voltage based on the crest voltage.

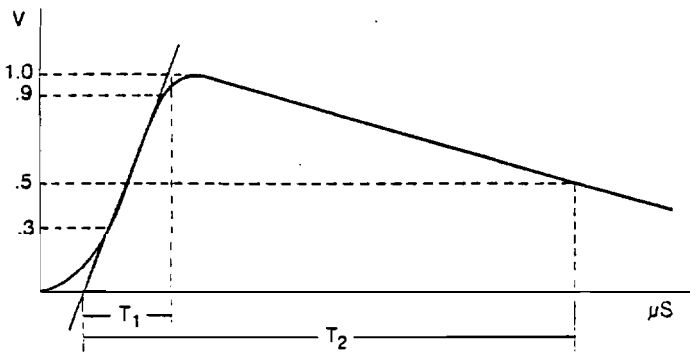

FIGURE VII.5 The generalized wave shape of induced voltages.

The comparison of measured and calculated induced voltage waveshapes has been studied in [4], Figure VII.6. The results show that the amplitude and general characteristics of the initial component are similar. The second peak in the measured wave tail, as the author explained, may

be caused by a leader branch.

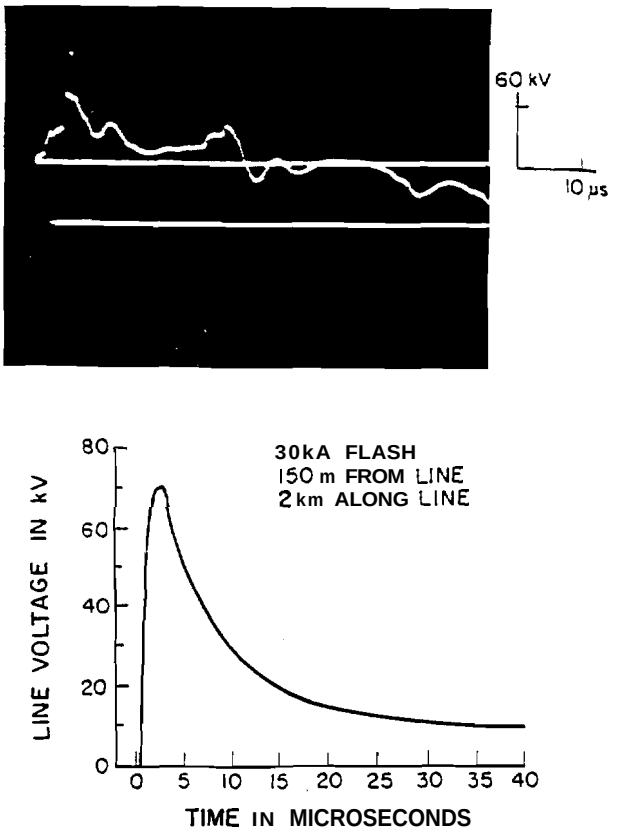

FIGURE VII.6 **Comparison of measured and calculated induced** surge **waveshapes.**

VII.4 Lightning damages on overhead distribution lines

Compared to the overvoltages caused by direct strokes, the magnitudes of induced voltages are usually lower. In transmission systems, the insulation is generally sufficient enough not to be endangered by induced voltages. However, distribution systems in which the insulation level is low, induced voltages are hazardous. When the induced voltage caused by lightning exceeds the strength of the insulation, a line flashover results, causing either temporary faults or disruption of services to customers. Furthermore, induced voltages generated on lines may travel along the line and into transformers (some distribution transformers are connected directly to the overhead lines) or substations, and may cause the insulation of the apparatus to break down, leading to immediate or eventual failure.

The place at which the most dangerous induced voltage occurs is still not quite understood. Some theoretical analyses indicate that the maximum value of induced voltage is obtained at the point on the line which is nearest to the lightning stroke[1]. However, experimental studies show the induced voltages are most dangerous at the ends of the distribution lines, and :must more dangerous at the poles branching the line than those at the neighboring poles[2].

VII.5 Methods to improve the lightning performance

VII.5.1 Increasing insulation level

The line flashover occurs when the insulation level is lower than the induced voltage. An increase of the insulation, namely an increase of the capability of insulation to the withstand overvoltage, will decrease dramatically the number of lightning faults, as shown in Figure VII.7[4]. One of most commonly used methods is wooden poles. Wood, even in wet conditions, acts as an insulator for lightning surges. The flashover voltage of wood may be estimated as 3kV/cm. Figure VII.8 gives the impulse withstand values of the combination of an insulator and wood [1]. It shows that if the wood length is enough to produce a withstand overvoltage greater than the insulator, the wood alone determines the insulation level.

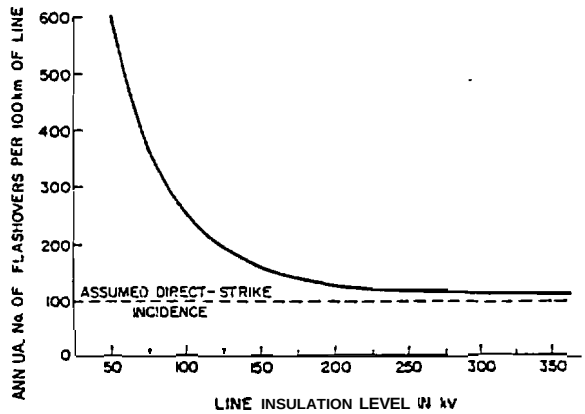

FIGURE VII.7 Calculation variation of annual distribution line flashover rate as a function of insulation level for ground-flash incidence of 7.5 per km2 per year.

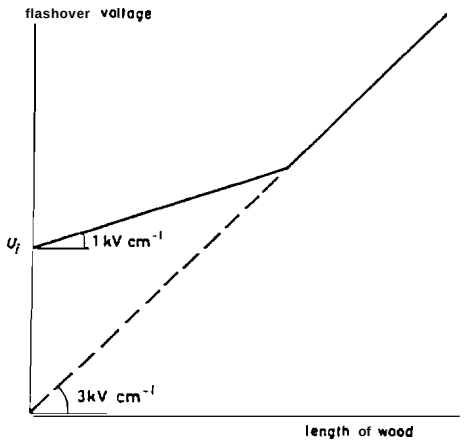

FIGURE VII.8 **Estimation of the flashover voltage of wood.**

(U_i = flashover voltage of insulator)

VII.5.2 Installation with earth wires

The earth wires have been used on distribution systems to suppress induced voltages. An earth wire can be installed either above the distribution lines or below them. Induced voltage amplitudes may be reduced by about 30 percent in the presence of an overhead earth wire and an underslung earth wire can give a reduction of about 20 percent[6]. The number of flashovers per annum for a given line length may be considerably reduced by using overhead shield wires earthed at every pole, when the pole footing resistances are less than about 25 ohms[6]. The effects of an earth wire are shown in Figure VII.9 [6].

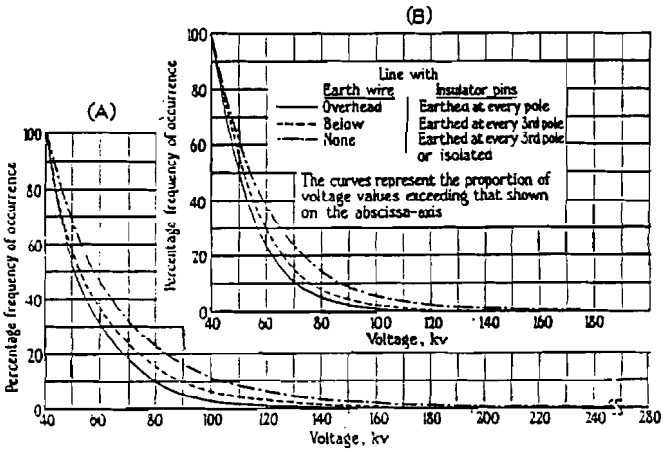

FIGURE VII.9 **Frequency distribution of induced voltages.**

(A) Due to strokes to open ground
(B) Due to strokes to earthed objects

VII.5.3 Installation with lightning arresters

The function of a lightning arrester is to limit high transient overvoltages to save values. A lightning arrester provides a path for the lightning current to flow into the ground, so that high voltage will not appear. In normal conditions a arrester is a very poor conductor so the power current can not flow through it. When a lightning induced voltage appears it becomes a good conductor and a good by-pass for lightning current The actual protective effects of lightning arresters and overhead earth wires have been compared in [2]. For 6.6 kV distribution lines, the protective effect of latter which have 3.5 ground points per km are the same or greater than that of the former of three installations per km.

VII.6 Summary

The lightning flash is a process of charge and discharge between the thundercloud and the ground or earthed objects. Usually the characteristic of lightning surge currents is high amplitude and short duration. For overhead distribution lines indirect lightning strokes are considered a significant problem because of their high frequency of occurrence. The induced voltage caused by indirect strokes is also an impulse with high amplitude. It propagates along lines in the form of a traveling wave. When the induced voltage exceeds the withstand voltages of the system insulation, insulation failure can result unless adequate overvoltage protection is provided. The useful methods to improve lightning performance on overhead distribution lines are: increasing the insulation level, using an overhead earth wire, or installing lightning arresters.

References

[1] S. Rusck, "Protection of *Distribution* Lines", Chapter 23, book on "Lightning - Volume 2", edited by R.H. Golde, Academic Press, 1977.

[2] K. Uehara, "*Investigation* of Lightning Damages on Distribution Lines", IEEE Transactions on Power Apparatus and Systems, Vol. PAS-87, pp1018-1025, April 1968.

[3] K. Denno, "High Voltage *Engineering* in Power System", CRC Press, 1992.

[4] A.J. Eriksson, "Lightning - Induced Overvoltages on Overhead Distribution lines", IEEE Transactions on Power Apparatus and Systems, Vol. PAP-101, No. 4 April 1982.

[5] J.H. Gosden, "Lightning *and* distribution *systems* - the nature of *the* problem", Conference on Lightning and the Distribution system, 17-18 January 1974.

[6] R. H. Golde, "*Lightning* Surge on Overhead Distribution Lines Caused by Indirect and Direct *Lightning* Strokes", AIEE Transactions, pp437-447, Vol. 73, 1954.

[7] A. J. Eriksson, D.V. Meal, "*Lightning* Performance and *Overvoltage* Surge Studies on a Rural Distribution Line", Proc. IEE, Vol. 129, Pt. C, March 1982, pp.59-69.

[8] E. Beck, "Lightning Protection For Electric System", McGRAW-HILL Hook Company, New York,1954.

[9] R. Rudenberg, "Electrical Shock Waves in Power Systems", Harvard University Press, Cambridge, 1968

[10] J.S.Cliff, "Insulation Coordination", Chapter 24, book on "Lightning - Volume 2", edited by R.H. Golde, Academic Press, 1977.